Contrib Mineral Petrol (2003) 145: 25–46
DOI 10.1007/s00410-002-0429-7

ORIGINAL PAPER

Balz S. Kamber · Kenneth D. Collerson
Stephen Moorbath · Martin J. Whitehouse

# Inheritance of early Archaean Pb-isotope variability from long-lived Hadean protocrust

Received: 1 March 2002 / Accepted: 28 October 2002 / Published online: 7 January 2003


**Abstract** Comparison of initial Pb-isotope signatures of several early Archaean (3.65–3.82 Ga) lithologies (orthogneisses and metasediments) and minerals (feldspar and galena) documents the existence of substantial isotopic heterogeneity in the early Archaean, particularly in the $^{207}Pb/^{204}Pb$ ratio. The magnitude of isotopic variability at 3.82–3.65 Ga requires source separation between 4.3 and 4.1 Ga, depending on the extent of U/Pb fractionation possible in the early Earth. The isotopic heterogeneity could reflect the coexistence of enriched and depleted mantle domains or the separation of a terrestrial protocrust with a $^{238}U/^{204}Pb$ ($\mu$) that was ca. 20–30% higher than coeval mantle. We prefer this latter explanation because the high-$\mu$ signature is most evident in metasediments (that formed at the Earth's surface). This interpretation is strengthened by the fact that no straightforward mantle model can be constructed for these high-$\mu$ lithologies without violating bulk silicate Earth constraints. The Pb-isotope evidence for a long-lived protocrust complements similar Hf-isotope data from the Earth's oldest zircons, which also require an origin from an enriched (low Lu/Hf) environment.

A model is developed in which ≥3.8-Ga tonalite and monzodiorite gneiss precursors (for one of which we provide zircon U-Pb data) are not mantle-derived but formed by remelting or differentiation of ancient (ca. 4.3 Ga) basaltic crust which had evolved with a higher U/Pb ratio than coeval mantle in the absence of the subduction process. With the initiation of terrestrial subduction at, we propose, ca. 3.75 Ga, most of the ≥3.8-Ga basaltic shell (and its differentiation products) was recycled into the mantle, because of the lack of a stabilising mantle lithosphere. We argue that the key event for preservation of all ≥3.8-Ga terrestrial crust was the intrusion of voluminous granitoids immediately after establishment of global subduction because of complementary creation of a lithospheric keel. Furthermore, we argue that preservation of ≥3.8-Ga material (in situ rocks and zircons) globally is restricted to cratons with a high U/Pb source character (North Atlantic, Slave, Zimbabwe, Yilgarn, and Wyoming), and that the Pb-isotope systematics of these provinces are ultimately explained by reworking of material that was derived from ca. 4.3 Ga (i.e. Hadean) basaltic crust.

B.S. Kamber (✉) · K.D. Collerson
Advanced Centre for Queensland University Isotope Research Excellence (ACQUIRE), University of Queensland, 4072 Brisbane, Queensland Australia
E-mail: kamber@earth.uq.edu.au

S. Moorbath
Department of Earth Sciences, University of Oxford, Oxford, OX1 3PR, UK

M.J. Whitehouse
Laboratory of Isotope Geology, Swedish Museum of Natural History, Box 50007 104 05 Stockholm, Sweden

Editorial responsibility: A. Hofmann

## Introduction

In a common Pb diagram, initial isotope compositions of terrestrial continental rocks form a broad, concave array that is most clearly defined by samples ca. 2.5 to ca. 1.5 Ga in age (Fig. 1). The wide dispersal in $^{207}Pb/^{204}Pb$ at a given $^{206}Pb/^{204}Pb$ is *prima facie* evidence that long-lived (>0.5-Ga) sources with different $^{238}U/^{204}Pb$ ($\mu$) existed in the crust-mantle system. Because of the rapid decay of $^{235}U$ (only ca. 1% of the original inventory remains today), continued differentiation into crust and mantle reservoirs is now no longer capable of producing a wide range of $^{207}Pb/^{206}Pb$ ratios. Rather, the wide $^{207}Pb/^{206}Pb$ dispersal presently observed reflects the fact that the mean age of exposed upper continental crust is 2–2.5 Ga, as indicated by Nd-isotopes (e.g. Goldstein and Jacobsen 1987). The large initial Pb-isotope variability is thus inherited from a time when more $^{235}U$ existed. The post-Archaean Pb-isotope evolution of the crust-mantle ensemble is best understood in terms of recycling of U and Pb from the crust into the mantle (e.g. Kramers and Tolstikhin 1997).

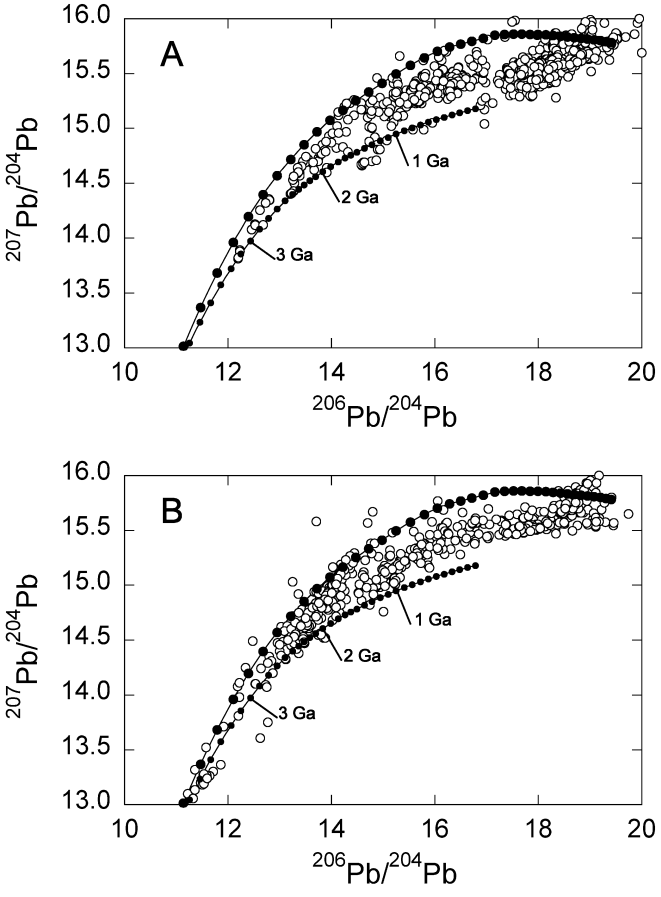


**Fig. 1** Pb-isotope diagrams showing initial isotope compositions (*open circles*) recorded in ores (**A**) and leached feldspars (**B**). Data compilation by Kramers and Tolstikhin (1997) based on USGS Pb-isotope database, supplemented for this study with feldspar data from Sultan et al. (1992); Neymark et al. (1994); Hemming et al. (1996,2000); Van Wyck and Johnson (1997); Kamber and Moorbath (1998); Möller et al. (1998); Qiu and McNaughton (1999); De et al. (2000); Bodet and Schärer (2001); Klötzli et al. (2001); and Cheong et al. (2002). The majority of data plot between the 'old upper crust' (*curve connecting large solid circles*) and 'young lower crust' (*curve connecting small solid circles*) evolution curves modelled by Kramers and Tolstikhin (1997)

The chief effects of these processes are to reduce the difference in $^{207}Pb/^{206}Pb$ between the mantle and crustal reservoirs, to decrease the modern $^{232}Th/^{238}U$ ($\kappa$) of the Mid-Ocean-Ridge Basalt (MORB)-source mantle and to gradually increase the upper crustal $\kappa$.

At the other end of the time scale, the extent of U/Th/Pb fractionation on the early Archaean Earth is still poorly understood, but evidence has long been published that by 3.7 Ga considerable differences in $^{207}Pb/^{204}Pb$ at a given $^{206}Pb/^{204}Pb$ already existed between chemical sediments and gneisses of magmatic origin (orthogneisses). Moorbath et al. (1973) observed in the early Archaean rocks from West Greenland that the difference in calculated source $\mu$ indicates "different immediate precursors for these two very different rock formations". Since then, additional observations from other Isua Greenstone Belt (IGB) lithologies in West Greenland have substantiated this early finding (Frei and Rosing 2001; Kamber et al. 2001), indicating that crustal and/or mantle sources remained isolated for extended periods of time during the early Archaean and possibly the Hadean (i.e. >4.0 Ga ago). The geodynamic significance of source material isolation in the early Earth is difficult to evaluate in the absence of direct constraints on the extent of U/Th/Pb fractionation that could have been generated by early Archaean or Hadean processes. Kamber et al. (2001) showed that the difference in documented ca. 3.7-Ga initial Pb-isotope ratios between orthogneisses and chemical sediments requires sediment source isolation for ca. 0.5 Ga if U/Pb fractionation was similar to that presently observed within the crust. Alternatively, if U/Pb fractionation was more extreme, the relatively large isotopic difference could be generated within as little as 100 Ma. The latter possibility needs to be considered because many lunar samples appear to have been derived from sources with exceedingly variable but generally high U/Pb (Nyquist and Shih 1992).

Here we report an extensive set of new Pb-isotope data (whole rock and feldspar) for ca. 3.8-Ga tonalitic gneisses and amphibolites from the North Atlantic Craton, as well as a compilation of previously published and unpublished Pb-isotope data for a variety of lithologies, including Pb ores, of the 3.7- to 3.8-Ga IGB. These data define an unexpectedly large variation in interpreted initial isotope ratios, providing incontrovertible evidence that strong U/Pb fractionation occurred perhaps as far back as the Hadean. We explore whether the isotope array requires a multitude of source histories or whether an evolution model can be derived which operates with only one depleted and one enriched end-member. Finally, we discuss implications for terrestrial Pb-isotope models, which aim at explaining the present-day isotope composition of silicate Earth reservoirs (plumbotectonics) and argue that the early Archaean record implies existence of a long-lived Hadean protocrust.

## Sample strategy in relation to field geology and previous studies

The Archaean Itsaq gneiss terrain in western Greenland is the largest, best-preserved, and most widely studied expanse of early Archaean rocks known on Earth. A smaller equivalent of these gneisses is exposed in the Hebron-Saglek segment of the Archaean gneisses in northern Labrador. Both areas form part of the North Atlantic Craton, which was contiguous prior to the opening of the Labrador Sea. These old gneiss complexes are predominantly composed of trondhjemitic, tonalitic and granodioritic (TTG) gneisses in which enclaves of supracrustal rocks (both metasediments and metavolcanic rocks) and older orthogneisses are found. In West Greenland, a special opportunity exists to study a large, well-preserved sequence of supracrustal rocks in the IGB, which contains a large variety of lithologies.

The best evidence for genuine, relatively undisturbed, 3.8-Ga continental crust has recently been published by Nutman et al. (1999) who described the geochronology of a gneiss complex south of the IGB. This complex (Fig. 2) has not been formally named, although it forms part of the regional Itsaq gneiss complex (Nutman et al. 1996, 1999). For the sake of clarity we here refer informally to this gneiss terrain as SOI (south of Isua) to distinguish it from other gneiss terrains in the region as a whole, and we refer to the studied rocks as SOI gneisses, SOI amphibolites, etc. In an attempt to substantiate claims for genuine 3.8-Ga magmatic precursors to these gneisses we present new ion-probe U-Pb zircon dates, although the main aim of our analytical effort was to reconstruct the source history of these and similar gneisses from northern Labrador using Pb-isotope data of separated feldspar. Below we describe in more detail the geological context of the studied samples.

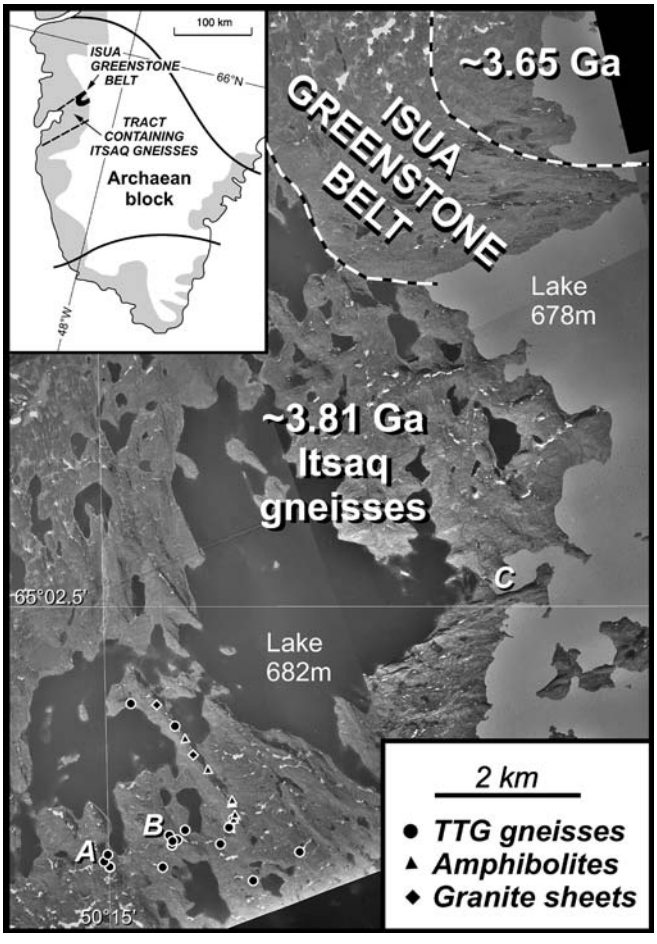


**Fig. 2** Mosaic of aerial photographs of the low strain, ca. 3.81-Ga Itsaq gneiss terrain immediately SW of the Isua Greenstone Belt (*IGB*) which is delineated by *dashed lines*. *Inset* shows location of the IGB on a map of southern Greenland. Sample localities referred to in this paper are indicated, together with localities *A*, *B* and *C* of Nutman et al. (1999)

## Greenland

In this paper, Pb-isotope data are presented and discussed for three principal early Archaean rock sequences from within the so-called Itsaq gneiss complex (Nutman et al. 1996) of southern West Greenland. These are (1) calc-alkaline (TTG) orthogneisses, still widely referred to as Amîtsoq gneisses, from the Godthaabsfjord region along, and adjacent to, the coastal province south and east of Nuuk; (2) calc-alkaline (TTG) orthogneisses from the SOI area immediately south of the IGB, which has only recently begun to be investigated in earnest. Significantly, these gneisses show both similarities and differences to the Godthaabsfjord gneisses and also to the orthogneisses to the north of (within) the arcuate IGB; and (3) the IGB itself, some 150 km north-east of Nuuk, comprising metamorphosed volcanic and sedimentary lithologies some of which host minor sulphide mineralisation, including galena with the least radiogenic terrestrial Pb so far known.

### *Godthaabsfjord region gneisses*

Since the early 1970s, much has been published about many aspects of these orthogneisses, of which their geochronology is the most relevant here. There is general agreement for a major period of emplacement of their magmatic precursors at ca. 3.65 Ga (e.g. Kamber and Moorbath 2000; McGregor 2000). However, debate continues on whether U-Pb zircon dates extending up to 3.90 Ga (Nutman et al. 1996, 2000) represent the magmatic protolith age (e.g. Nutman et al. 2001), or represent zircons inherited from older source regions (Whitehouse et al. 1999, 2001). In the strongly banded TTG gneisses, the additional possibility exists that genetically unrelated igneous rocks, ranging in age from 3.9 to 3.6 Ga, could have been intercalated as narrow bands.

The Godthaabsfjord region gneisses have long been known to contain the least radiogenic terrestrial silicate leads so far discovered (e.g. Black et al. 1971; Gancarz and Wasserburg 1977). Building on all previous work, combined with new analyses, Kamber and Moorbath (1998) tabulated and regressed the available Pb-isotope data from the Godthaabsfjord gneisses and concluded that all analysed whole rock and feldspar samples pointed to an age of ca. 3.65 Ga, even for some which contained zircons with significantly older portions. The Pb-isotope data for whole rocks and feldspars used in the figures and elsewhere are the ones listed in Table 1 of Kamber and Moorbath (1998) and represent some of the most typical gneiss units in the Godthaabsfjord region.

### *South-of-Isua (SOI) gneisses*

This is an extensive terrain (Fig. 2) of varied, amphibolite-facies, TTG-type gneiss with numerous, large (up to several hundred meters) enclaves of older ultramafic rocks, metagabbros, layered amphibolites ($\pm$garnet) with interlayers of metamorphosed BIF and thin felsic

**Table 1** Pb-isotope data compilation of Isua Greenstone Belt (*IGB*) lithologies and galenas. Numbers in columns entitled "Source" refer to analysts or data source: *1* previously unpublished Oxford data by Roy Goodwin, Stephen Moorbath and Paul Taylor; *2* data from Moorbath et al. (1975); *3* previously unpublished Oxford data by Roy Goodwin, Stephen Moorbath and Martin Whitehouse; *4* previously unpublished Brisbane TIMS data by Balz Kamber and Peter Appel; *5* data from Richards and Appel (1987); *6* data from Appel et al. (1978); *7* data from Frei and Rosing (2001). All previously unpublished data are normalised relative to recommended NBS SRM 981 ratios of Todt et al. (1996). Accuracy (2 sigma) of the three Pb-isotope ratios is better than 0.25, 0.30 and 0.42% in the Oxford data set, and better than 0.17, 0.23 and 0.31% in the Brisbane data set

| Sample | $^{206}Pb/^{204}Pb$ | $^{207}Pb/^{204}Pb$ | $^{208}Pb/^{204}Pb$ | Source |
|---|---|---|---|---|
| 3.81-Ga felsic "volcanogenicmetasediment boulders" | | | | |
| 248412 | 16.236 | 14.803 | 37.700 | 1 |
| 248413 | 12.285 | 13.620 | 32.501 | 1 |
| 248414 | 11.842 | 13.420 | 32.001 | 1 |
| 248415 | 12.133 | 13.477 | 32.233 | 1 |
| 248416 | 13.169 | 13.838 | 33.356 | 1 |
| 248418 | 14.612 | 14.285 | 35.115 | 1 |
| 248419 | 14.121 | 14.186 | 34.412 | 1 |
| 248426 | 14.510 | 14.288 | 36.054 | 1 |
| 248431 | 13.666 | 13.993 | 33.898 | 1 |
| 248432 | 14.129 | 14.187 | 33.359 | 1 |
| 158493 | 13.109 | 13.671 | 33.550 | 2 |
| 158536 | 12.301 | 13.536 | 32.534 | 2 |
| 158537 | 12.238 | 13.541 | 31.941 | 2 |
| 158538 | 12.146 | 13.536 | 32.476 | 2 |
| SM/GR/93/9 | 13.529 | 13.844 | 33.801 | 3 |
| SM/GR/93/21 | 12.495 | 13.550 | 33.211 | 3 |
| Matrix of 3.81-Ga"volcanogenic metased. boulders" | | | | |
| 248421 | 14.696 | 14.353 | 35.980 | 1 |
| 248422 | 14.344 | 14.168 | 35.102 | 1 |
| 248423 | 14.278 | 14.130 | 35.160 | 1 |
| 248424 | 13.045 | 13.694 | 33.270 | 1 |
| 248425 | 12.864 | 13.627 | 33.308 | 1 |
| 248428 | 13.201 | 13.840 | 33.636 | 1 |
| 248429 | 12.560 | 13.617 | 32.842 | 1 |
| 248430 | 12.456 | 13.546 | 32.704 | 1 |
| 248433 | 14.046 | 14.133 | 34.461 | 1 |
| 3.71-Ga felsic "volcanogenicmetasediments" | | | | |
| 248481A | 24.526 | 17.582 | 46.121 | 1 |
| 248481B | 17.499 | 15.295 | 38.331 | 1 |
| 248481C | 23.033 | 17.071 | 44.546 | 1 |
| 248481D | 15.232 | 14.523 | 35.670 | 1 |
| 248481E | 15.965 | 14.766 | 36.435 | 1 |
| 248481F | 16.773 | 15.180 | 37.018 | 1 |
| 248481G | 16.958 | 15.224 | 37.431 | 1 |
| 248481H | 19.058 | 15.960 | 39.917 | 1 |
| 248481J | 15.708 | 14.847 | 35.867 | 1 |
| 248481K | 17.260 | 15.439 | 37.362 | 1 |
| 248481L | 20.062 | 16.170 | 40.978 | 1 |
| 248481M | 22.266 | 16.882 | 43.570 | 1 |
| SM/GR/93/59 | 14.916 | 14.416 | 35.477 | 3 |
| 3.71-Ga garnet-mica schists(single locality) | | | | |
| 248484A | 17.400 | 15.442 | 38.178 | 1 |
| 248484B | 16.927 | 15.352 | 37.773 | 1 |
| 248484C | 17.122 | 15.461 | 38.055 | 1 |
| 248484D | 17.691 | 15.535 | 38.640 | 1 |
| 248484E | 16.499 | 15.187 | 37.081 | 1 |
| 248484F | 15.404 | 14.788 | 35.293 | 1 |
| 248484G | 17.886 | 15.615 | 39.088 | 1 |
| 248484H | 16.146 | 15.055 | 36.094 | 1 |
| 248484J | 15.864 | 14.964 | 36.202 | 1 |
| 248484K | 17.569 | 15.518 | 38.039 | 1 |
| 248484L | 14.536 | 14.439 | 34.782 | 1 |
| 3.71-Ga garnet-mica schists(eastern IGB) | | | | |
| SM/GR/93/56 | 16.072 | 15.130 | 36.992 | 3 |
| SM/GR/93/57 | 17.719 | 15.423 | 38.664 | 3 |
| 3.71-Ga garnet-mica schists(eastern IGB) continued | | | | |
| SM/GR/93/58 | 16.742 | 15.156 | 37.076 | 3 |
| SM/GR/93/10 | 12.796 | 13.730 | 32.522 | 3 |
| SM/GR/93/11 | 12.262 | 13.619 | 31.838 | 3 |
| SM/GR/93/13 | 12.315 | 13.625 | 31.935 | 3 |
| SM/GR/93/15 | 13.601 | 13.913 | 33.169 | 3 |
| SM/GR/93/22 | 12.178 | 13.395 | 32.158 | 3 |
| SM/GR/93/28 | 12.187 | 13.609 | 31.853 | 3 |
| SM/GR/93/33 | 12.031 | 13.466 | 31.914 | 3 |
| SM/GR/93/75 | 12.680 | 13.761 | 32.528 | 3 |
| SM/GR/93/76 | 13.719 | 14.056 | 34.007 | 3 |
| "Tourmaline boulder" in garnet-micaschists | | | | |
| 248483B | 14.161 | 14.250 | 33.835 | 1 |
| 248483E | 13.963 | 14.213 | 33.485 | 1 |
| 248483F | 14.302 | 14.325 | 34.067 | 1 |
| 248483G | 14.583 | 14.323 | 34.076 | 1 |
| 248483H | 14.413 | 14.299 | 34.624 | 1 |
| 248483J | 14.702 | 14.385 | 34.537 | 1 |
| Galenas (unpublished data) | | | | |
| SM/GR/93/18A | 11.483 | 13.372 | 31.445 | 1 |
| SM/GR/93/18B | 11.440 | 13.368 | 31.473 | 1 |
| SM/GR/93/18C | 11.475 | 13.358 | 31.408 | 1 |
| 215720 | 11.103 | 13.014 | 31.366 | 3 |
| 215730 | 11.086 | 12.984 | 31.281 | 3 |
| HKS 450168A | 11.034 | 12.898 | 31.035 | 3 |
| HKS 450168B | 11.025 | 12.891 | 30.990 | 3 |
| HKS 450168C | 11.022 | 12.882 | 30.978 | 3 |
| HKS 450168D | 11.024 | 12.917 | 31.093 | 4 |
| HKS 462749 | 11.023 | 12.886 | 31.003 | 4 |
| HKS 462750 | 11.039 | 12.913 | 31.095 | 4 |
| HKS 462751 | 11.024 | 12.888 | 31.006 | 4 |
| HKS 462752 | 11.029 | 12.899 | 31.042 | 4 |
| HKS 462753 | 11.031 | 12.895 | 31.019 | 4 |
| HKS 462759 | 11.121 | 12.984 | 31.072 | 4 |
| HKS 462762 | 11.135 | 12.998 | 31.113 | 4 |
| HKS 462768 | 11.141 | 13.019 | 31.184 | 4 |
| HKS 462776 | 12.228 | 13.767 | 32.065 | 4 |
| HKS 462754 | 12.478 | 13.707 | 32.070 | 4 |
| HKS 467256 | 12.200 | 13.663 | 31.823 | 4 |
| HKS 462757 | 12.136 | 13.637 | 31.756 | 4 |
| Galenas (published data) | | | | |
| 539 | 11.176 | 13.047 | 31.130 | 5 |
| 540 | 11.311 | 13.147 | 31.265 | 5 |
| 541 | 11.195 | 13.062 | 31.171 | 5 |
| 542 | 11.266 | 13.110 | 31.198 | 5 |
| 542 | 11.272 | 13.121 | 31.225 | 5 |
| 543 | 11.275 | 13.124 | 31.230 | 5 |
| 2946 | 11.434 | 13.345 | 31.424 | 6 |
| 2954 | 11.428 | 13.335 | 31.383 | 6 |
| 2926 | 11.314 | 13.158 | 31.301 | 6 |
| 2926 | 11.326 | 13.175 | 31.335 | 6 |
| 2966 | 11.146 | 13.025 | 31.148 | 6 |
| 2966 | 11.151 | 13.037 | 31.179 | 6 |
| 2966 | 11.164 | 13.052 | 31.216 | 6 |
| 460000–1 | 11.022 | 12.887 | 30.987 | 7 |
| 940001 | 11.131 | 13.004 | 31.126 | 7 |

bands of unknown origin. The entire assemblage is traversed by mostly discordant, amphibolite-facies, mafic dykes, regarded as equivalent to the mid-Archaean Ameralik dykes elsewhere in the Itsaq gneiss complex. SOI TTG gneisses range from strongly banded (i.e. typical grey gneiss) to homogeneous varieties. The homo-

geneous gneisses are equigranular, but no *bona fide* igneous textural features are preserved, indicating that amphibolite-facies recrystallisation occurred under low strain. There is probably a greater proportion of homogeneous gneisses here than anywhere else in the Itsaq gneiss complex, as already noted by Nutman et al. (1999). Younger pre- and post-dyke granitoid sheets and pegmatites are locally present. There is evidence for pre- and post-dyke metamorphism and deformation.

Nutman et al. (1996, 1999) have convincingly shown that oscillatory-zoned prismatic grains with simple age structures dominate zircon populations from SOI tonalites and quartz-diorites, yielding single-population dates of mainly 3818 ± 8 Ma. This is in strong contrast to the geochronologically and structurally much more complex zircon populations of the Godthaabsfjord region, as well as the well-preserved, low-strain tonalite gneisses north of the IGB (Fig. 2), which have only yielded zircon U-Pb dates of 3.65–3.70 Ga, and not 3.8 Ga (Nutman et al. 1996). Zircon U-Pb ages from SOI gneisses thus yield the best evidence so far for the existence of in-situ ≥3.8-Ga-old granitoid crust in the Itsaq gneiss complex.

Samples for further zircon U-Pb work (presented in this study) and for a comprehensive Pb-isotope survey (the main purpose of this paper) were collected by S. Moorbath and M.J. Whitehouse. We have closely followed the paper by Nutman et al. (1999) and concentrated sampling efforts on the outcrops either at, or surrounding (within ca. 2 km), their localities, where there are numerous fine exposures of homogeneous tonalitic gneisses, with or without biotite foliation, traversed by occasional discordant Ameralik dykes. The geology of the relevant localities (marked A and B) is discussed in detail by Nutman et al. (1999).

Seven samples of enclaves of layered amphibolites and garnet-amphibolites analysed for Pb-isotopes also come from outcrops within 1–2 km of localities A and B, whilst samples 409019 and 409030 consist of thin (ca. 20-cm), concordant, fine-grained granitoid sheets interlayered in the amphibolites.

### *Isua Greenstone Belt (IGB)*

The oldest known, early Archaean sedimentary and volcanic rocks, as well as their mostly intense (amphibolite facies) metamorphism and deformation, have been closely studied for some 30 years. Opinions regarding the protoliths and the tectonic structure of the IGB are still evolving, as can be seen by comparing and contrasting, for example, the views of Nutman et al. (1984) with those of Fedo et al. (2001) and Myers (2001). There is also ongoing debate regarding the absolute ages of the various lithologies, although most investigators (ourselves included) agree that direct U-Pb zircon evidence by Nutman et al. (1997) points to a bimodal age distribution, with the majority of dated lithologies clustering tightly around 3.71 Ga in age, and a minority of directly dated lithologies extending to an age of 3.81 Ga. A model age of 3.81 Ga has also been claimed to explain the least radiogenic Pb-isotope ratios of IGB galena (Frei and Rosing 2001). There is also evidence (from zircons in possible metasediments; Nutman et al. 1997) for the (former) existence of even older rocks of up to 3.9 Ga.

The Pb-isotope data for the IGB, which are tabulated (Table 1) and plotted in this paper, are based on representative (metamorphic) lithologies from the eastern sector of the belt, collected by S. Moorbath and P.N. Taylor. Within the framework of Nutman et al.'s (1997) chronology, our selection of rocks includes representatives of both the 3.81- and the 3.71-Ga age group: BIF; carbonates; metapelitic garnet-mica (± staurolite, ± amphibole) schists probably derived from mafic, volcanogenic sediments; a tourmaline-bearing quartzo-feldspathic fragment enclosed within the metapelites; quartzo-feldspathic schists, probably derived from felsic, volcanogenic sediments; and interlayered quartzo-feldspathic rocks possibly derived from highly tectonised, metasomatised granitoid rocks (see Myers 2001). Kamber et al. (1998) obtained a whole-rock Sm-Nd regression age of 3742 ± 49 Ma for the garnet-mica schist suite, which agrees within error with the 3.71-Ga U-Pb zircon ages obtained for metasedimentary lithologies by Nutman et al. (1997).

Galena is found as small disseminations, patches and veins, together with other sulphides, within different lithologies of the IGB. The sulphide occurrences are not primary features of the lithologies but have formed (or were remobilised) during metamorphic events (Frei et al. 1999). All samples, except one, for which we present new data were collected by geologists of the Nunaoil Company and by Peter Appel of the Geological Survey of Denmark and Greenland. The exception is SM/GR/93/18, collected by S. Moorbath, which occurs as a scattered dissemination of galena in recrystallised chert at a locality in the eastern sector of the IGB, famous for the occurrence of ornamental fuchsite-quartzite. The uniquely (i.e. terrestrial) unradiogenic character of Pb in several IGB galenas was discovered by Appel et al. (1978), and further investigated by Richards and Appel (1987) and Frei and Rosing (2001).

## Labrador

Sample selection for the northern Labrador segment of the North Atlantic craton was based on relative chronology established in exposures of low-strain gneiss domains. Two different groups of gneisses were chosen for Pb-isotope analysis (whole rocks and feldspar separates). First, the Uivak I (hereafter simply called Uivak) TTG gneisses dominate the early Archaean Gneiss Complex in the Saglek-Hebron area (Collerson 1983a; Collerson et al. 1989; Schiøtte et al. 1989). These gneisses are considered broadly similar in age and character to the TTG gneisses of the Godthaabsfjord area in Greenland (Collerson et al. 1989). The best U-Pb igneous zircon age estimate for the Uivak gneisses is 3732 ± 6 Ma (Collerson 1983a; Schiøtte et al. 1989). Like

many Godthaabsfjord TTG gneisses, the euhedral, zoned, igneous Uivak zircons sometimes contain rounded cores of up to 3,863 ± 12 Ma, which were interpreted as inherited from pre-existing evolved rocks or from the melt source (Schiøtte et al. 1989). Although complicated by later metamorphic events, whole-rock Rb-Sr, Sm-Nd and Pb/Pb regression dates are compatible with the 3.73-Ga age estimate and indicate derivation from a slightly depleted (relative to chondrite) mantle source (Collerson 1983a). There is only minimal difference in radiogenic isotope systematics between undisturbed Uivak and Godthaabsfjord gneisses.

The second set of gneisses, termed Nanok gneisses, is of different character and of distinctive iron-rich monzodioritic composition. Along the southern shore of Tigigakyut Inlet, between Hebron and Saglek, Nanok gneisses occur as easily recognisable enclaves in relatively undeformed Uivak gneiss. One specimen of Nanok gneiss (from Big Island, Saglek Bay) has yielded zircon U-Pb dates of 3.92 and 3.81 to ca. 3.7 Ga (Collerson 1983a). Based on the relative chronology (i.e. the observation that the Nanok gneisses predate Uivak gneisses), the ca. 3.7-Ga date was interpreted as the time of incorporation of enclaves into Uivak magma. It is presently unresolved which of the older two dates (3.81 or 3.92 Ga) corresponds to the igneous emplacement age. Regardless, for the purpose of the present paper it is sufficient to note that Nanok gneisses predate the Uivak gneisses by at least 80 if not 190 Ma.

Collerson (1983b) used secondary Rb-Sr isochrons and mineral ages to reconstruct the polymetamorphic history of the Uivak gneisses. Sr-isotope homogenisation events, on the mineral and compositional layer scale (for banded gneisses), were recorded at 2.8, 2.5 and 1.8 Ga. The oldest of these homogenisation events is also evident from U-Pb systematics of rims that developed on igneous zircons (Collerson 1983a; Schiøtte et al. 1989).

## New U-Pb ion probe dates for SOI TTG gneiss

One sample of a typical, homogeneous SOI TTG gneiss (SM/GR/98/2) was collected during a reconnaissance visit in 1998 from a locality in the northern SOI gneiss terrain, ca. 4 km south of the IGB. We regard this sample as equivalent to Nutman et al.'s (1996) quartz-diorite sample 292128.

SIMS U-Th-Pb analyses were performed using a Cameca IMS1270 ion-microprobe located at the Nord-SIMS facility in Stockholm. Analytical details are given in the caption to Table 2. Results are reported in Table 2 and Fig. 3. Cathodoluminesence images of zircons from SM/GR/98/2 reveal relatively simple internal structures with concentric fine oscillatory zoning generally considered typical of magmatic growth (Fig. 3). This observation is in accord with that of Nutman et al. (1999) for zircons from their SOI terrain samples. In Fig. 3, $^{207}Pb/^{206}Pb$ ages exhibit a small spread along concordia with the highest ages > 3.8 Ga. Given the simplicity of internal structure revealed by the CL images, and the differences in replicate analyses on the same growth phase (Table 2), we consider that $^{207}Pb/^{206}Pb$ ages < 3.8 Ga most likely represent ancient Pb-loss. The five grains with highest ages yield a weighted average $^{207}Pb/^{206}Pb$ age of 3813 ± 10 Ma ($2\sigma$, MSWD = 2.9). These same five grains also yield a concordia age (Ludwig 1999) of 3,812 ± 14 Ma (MSWD of concordance = 4.5; decay constant errors included). These ages, however calculated, are within error of ages reported from the SOI terrain by Nutman et al. (1996, 1999) and we agree with the conclusion of these authors that this represents the age of the magmatic protolith to these rocks. In conclusion, our new zircon data agree with the observations of Nutman et al. (1999) of relatively simple, igneous internal structure of SOI TTG gneiss zircons, which is reflected in comparatively (to the Godthaabsfjord TTG gneisses) uniform age distribution clustering between 3.81 and 3.82 Ga. This age is regarded as the most likely time of crystallisation of the gneiss precursors.

## Pb-isotope results for TTG gneisses

Pb-isotope data for the SOI gneisses are presented in Table 3 and were obtained by multi-collector ICP-MS at the ACQUIRE Laboratory, University of Queensland. Analytical details are given in the table legend and followed closely those of Collerson et al. (2002). Pb-isotope data of the Labrador samples are listed in Table 4 and were obtained by TIMS in the Department of Earth Sciences of the University of California at Santa Cruz. Analytical details are given in the table legend and closely followed those of Palacz (1985).

### Whole rocks

Whole-rock Pb-isotope data for SOI gneisses are plotted according to field-derived relative chronology (Fig. 4A). The two granitoid sheets that occur structurally concordant within amphibolites contain the most radiogenic Pb and, because of their unknown absolute age, will not be considered further. The whole-rock data of the tonalite gneisses range from very unradiogenic to typical crustal values, but on average, they are significantly more radiogenic than 3.65-Ga Amîtsoq-type gneisses from the Godthaabsfjord region (Kamber and Moorbath 1998). Furthermore, there is significant scatter such that the apparent regression age of 3,706 Ma has a large uncertainty of 190 Ma (2 sigma). Note that the high MSWD of 31,782 obtained from the MC-ICP-MS data (using external precision rather than the smaller internal error) cannot be compared with that for data obtained by conventional (unspiked) thermal ionisation mass spectrometry, which would yield an MSWD at least 100 times lower for the same degree of scatter. While the regression date agrees within error with the U-Pb zircon age range of

**Table 2** Ion-microprobe U-Th-Pb data for zircons from sample SM/GR/98/2. Analytical parameters are identical to those reported by Whitehouse et al. (1999) and references therein. Errors on $^{207}Pb/^{206}Pb$ ratios are the raw counting statistic errors; Pb/U ratios are calibrated relative to the 1,065-Ma Geostandards zircon 91500 (Wiedenbeck et al. 1995) and contain a propagated (and dominant) error component from the pooled standard analyses (ca. 2.5% 1 sigma for this analytical session)

| Analysis ID | [U] (ppm) | [Pb] (ppm) | Th/U[a] | $f_{206}$[b] (%) | $^{206}Pb/^{204}Pb$ | $^{207}Pb/^{206}Pb$ | $^{206}Pb/^{238}U$ | $^{207}Pb/^{206}Pb$ age (Ma) | $^{206}Pb/^{238}U$ age (Ma) |
|---|---|---|---|---|---|---|---|---|---|
| 2b | 190 | 231 | 0.63 | 0.07 | 26,116 | 0.3630 ± 0.0011 | 0.7951 ± 0.0186 | 3,763 ± 5 | 3,774 ± 67 |
| 2a | 292 | 337 | 0.33 | 0.04 | 49,456 | 0.3684 ± 0.0008 | 0.7917 ± 0.0180 | 3,785 ± 4 | 3,761 ± 65 |
| 5b | 128 | 150 | 0.48 | 0.70 | 2,668 | 0.3696 ± 0.0020 | 0.7937 ± 0.0181 | 3,790 ± 9 | 3,787 ± 66 |
| 1d | 72 | 92 | 0.77 | (0.05) | 34,025 | 0.3704 ± 0.0013 | 0.8083 ± 0.0184 | 3,793 ± 5 | 3,819 ± 66 |
| 1c | 142 | 175 | 0.60 | 0.08 | 23,079 | 0.3734 ± 0.0009 | 0.7986 ± 0.0182 | 3,805 ± 4 | 3,786 ± 66 |
| 5a | 260 | 293 | 0.10 | 0.03 | 53,967 | 0.3745 ± 0.0010 | 0.8006 ± 0.0182 | 3,810 ± 4 | 3,793 ± 66 |
| 6a | 85 | 111 | 1.01 | (0.03) | 58,651 | 0.3757 ± 0.0014 | 0.7896 ± 0.0179 | 3,815 ± 6 | 3,752 ± 65 |
| 3a | 112 | 138 | 0.76 | 0.54 | 3,466 | 0.3758 ± 0.0016 | 0.7760 ± 0.0182 | 3,815 ± 6 | 3,718 ± 67 |
| 6c | 147 | 193 | 1.06 | 0.15 | 12,793 | 0.3779 ± 0.0009 | 0.7801 ± 0.0179 | 3,824 ± 4 | 3,722 ± 66 |

[a]Calculated from measured ThO intensity.
[b]Percentage of common Pb detected, calculated from measured $^{204}Pb$ assuming 0-Ma Stacey and Kramers (1975) model. Common Pb correction has not been applied for samples for which this number is in parentheses due to low $^{204}Pb$ counts.

3.80–3.82 Ga, it is obvious that the scatter about the regression reflects either substantial initial isotope heterogeneity or disturbance of the U/Pb ratios. We will argue later that these rocks were affected by late Archaean and early Proterozoic regional open-system events that changed their U/Pb ratios and disturbed their isochronous Pb-isotope systematics. Nevertheless, the least radiogenic datapoints (as well as the intercept of the regression line with mantle evolution models) are still difficult to reconcile with a 3.80- to 3.82-Ga mantle origin, because the data plot well above, and to the right of, such an old model age. A forced regression to 3.81 Ga yields much too young an intersection with the Kramers and Tolstikhin (1997) mantle evolution curve at 3,685 Ma. Pb-isotope ratios of the amphibolite gneisses do not plot substantially off the tonalite regression line (Fig. 4Aa), but have themselves insufficient spread for meaningful regression.

Similarly, the whole-rock data for the Labrador gneisses are not well aligned (Fig. 4B), but plot roughly along a similar trend to the SOI data. It is clear that the whole-rock data on their own cannot be used to evaluate claims for 3.80- to 3.82-Ga (SOI), 3.81- to 3.92-Ga (Nanok) and 3.73-Ga (Uivak) emplacement ages, nor can the data be used to infer probable source histories with any reasonable confidence.

## Feldspars

By comparison with the whole rocks, the feldspar Pb-isotope data are much better aligned in common Pb space. Pb-isotope ratios of (leached) feldspars are significantly less radiogenic than those of the whole rocks (Fig. 5). Data for the four main groups of rocks yield reasonably tight regression lines, which are readily identified as sec-

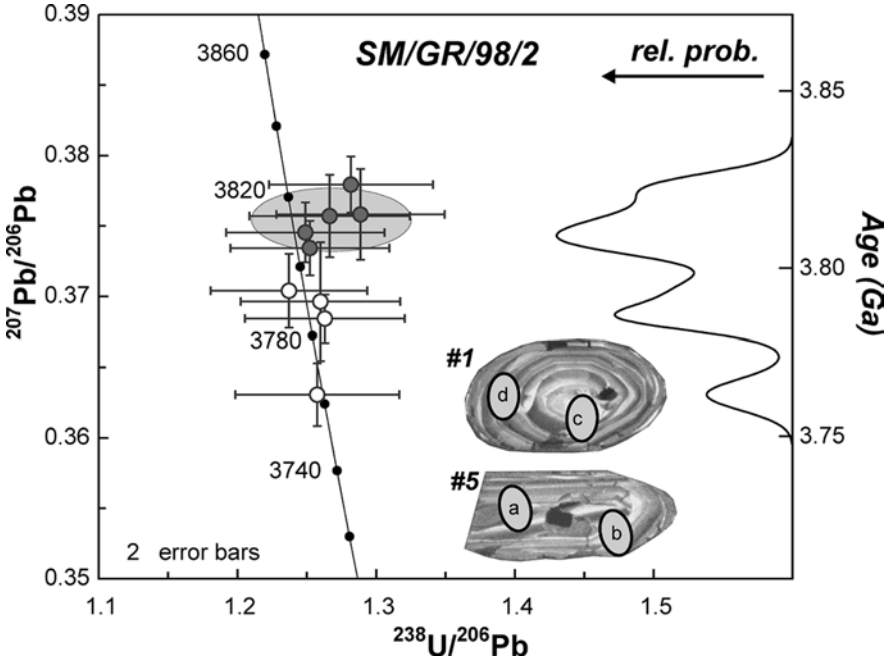


**Fig. 3** Inverse (Tera-Wasserburg) concordia diagram for SIMS analyses from SM/GR/98/2 (Table 2). Cumulative probability diagram of $^{207}Pb/^{206}Pb$ ratios is shown at *right-hand side* with the secondary y-axis indicating age. *Shaded ellipse* shows the concordia age of 3,812 ± 14 Ma (95% confidence) obtained from the five samples with the highest $^{207}Pb/^{206}Pb$ ratios. Inset cathodoluminescence images are shown for two typical zircon grains from this sample

**Table 3** Pb-isotope data for gneisses from SOI terrain. GPS localities use the WGS84 datum. Sample numbers (4090xx series) refer to the archives of the Geological Survey of Denmark and Greenland (GEUS). *Letters in parentheses* after the coordinates refer tolocalities studied by Nutman et al. (1999) and use the same designation. All samplescollected by S. Moorbath and M.J. Whitehouse. Feldspar (mainly plagioclase) mineral separates were obtained by magnetic and density separation and were washed three times in ultrapure water in an ultrasonic agitator. They were first leached for 24 h in 2 N HCl on a 100 ºC hotplate and then for 20 min in cold 14 N HF. Before final dissolution, the leached mineral separate was cleaned three times in ultrapure water. Reproducibility of leaching procedure was tested with sample 409010 and was found to be excellent. Total procedural blank remained below 22 pg and was insignificant. Multi-collector ICPMS mass spectrometric procedures followed closely those ofCollerson et al. (2002). Internal precision on all three ratios ofall samples was 3–8 times better than two-sigma external reproducibility of NBS SRM 981 ($n=114$), which yielded $^{206}Pb/^{204}Pb$ of 16.941 ($\pm 374$ ppm), $^{207}Pb/^{204}Pb$of 15.495 ($\pm 490$ ppm) and $^{208}Pb/^{204}Pb$ of 36.720 ($\pm 634$ ppm). For regression calculations, data points were assigned external errors whichwere always larger than internal precision

| Sample | Location | Whole rocks | | | | Feldspars | | |
|---|---|---|---|---|---|---|---|---|
| | (lat. N, long. W) | $^{206}Pb/^{204}Pb$ | $^{207}Pb/^{204}Pb$ | $^{208}Pb/^{204}Pb$ | | $^{206}Pb/^{204}Pb$ | $^{207}Pb/^{204}Pb$ | $^{208}Pb/^{204}Pb$ |
| TTG gneisses | | | | | | | | |
| SM/GR/98/2 | 65°02.70′, 50°08.36′ (C) | 12.010 | 13.308 | 34.957 | | 11.328 | 13.100 | 31.449 |
| 409001 | 65°00.761′, 50°13.625′(B) | 12.058 | 13.363 | 32.206 | | 11.507 | 13.224 | 31.323 |
| 409002 | 65°00.761′, 50°13.625′(B) | 12.863 | 13.747 | 32.606 | | 11.955 | 13.519 | 31.484 |
| 409003 | 65°00.761′, 50°13.625′(B) | 16.362 | 14.567 | 37.550 | | 12.121 | 13.579 | 31.760 |
| 409004 | 65°00.64′, 50°14.89′(A) | 12.966 | 13.723 | 32.366 | | 11.939 | 13.478 | 31.437 |
| 409005 | 65°00.64′, 50°14.89′(A) | 13.216 | 13.753 | 32.150 | | 11.891 | 13.417 | 31.358 |
| 409006 | 65°00.64′, 50°14.89′(A) | 12.498 | 13.549 | 32.030 | | 11.866 | 13.394 | 31.432 |
| 409007 | 65°00.64′, 50°14.89′(A) | 14.239 | 14.040 | 32.946 | | 12.249 | 13.617 | 31.445 |
| 409008 | 65°00.64′, 50°14.89′(A) | 11.848 | 13.303 | 32.445 | | 11.479 | 13.198 | 31.356 |
| 409010 | 65°00.64′, 50°14.89′(A) | 14.220 | 13.980 | 32.042 | | 12.361 | 13.635 | 31.485 |
| 409010 | | Separately leached aliquot | | | | 12.387 | 13.638 | 31.478 |
| 409011 | 65°00.80′, 50°13.75′(B) | 13.752 | 13.996 | 31.825 | | 12.188 | 13.639 | 31.332 |
| 409014 | 65°00.83′, 50°13.48′ | 12.547 | 13.713 | 32.068 | | 11.963 | 13.564 | 31.758 |
| 409015 | 65°00.83′, 50°13.48′ | 12.759 | 13.614 | 33.600 | | 11.739 | 13.342 | 31.582 |
| 409016 | 65°00.884′, 50°12.644′ | 15.118 | 14.640 | 33.351 | | 13.197 | 14.248 | 32.282 |
| 409021 | 65°00.754′, 50°13.703′ | 15.944 | 14.758 | 36.212 | | 13.282 | 14.219 | 32.718 |
| 409032 | 65°00.40′, 50°12.40′ | 15.449 | 14.853 | 35.656 | | 13.536 | 14.403 | 32.196 |
| 409033 | 65°00.70′, 50°12.90′ | 16.259 | 14.939 | 34.600 | | 13.344 | 14.337 | 31.969 |
| 409034 | 65°01.63′, 50°13.50′ | 13.137 | 13.700 | 33.787 | | 11.896 | 13.399 | 31.702 |
| 409035 | 65°01.83′, 50°14.21′ | 12.195 | 13.448 | 33.015 | | 11.617 | 13.275 | 31.500 |
| 409037 | 65°00.827′, 50°12.718′ | 13.584 | 14.007 | 33.550 | | 12.182 | 13.658 | 31.724 |
| 409038 | 65°00.820′, 50°12.729′ | 14.948 | 14.412 | 35.540 | | 12.797 | 13.926 | 32.215 |
| 409040 | 65°00.56′, 50°13.91′ | 12.391 | 13.594 | 32.538 | | 11.851 | 13.459 | 31.560 |
| 409042 | 65°00.691′, 50°14.821′ | 12.445 | 13.737 | 32.244 | | 12.037 | 13.624 | 31.715 |
| Amphibolites | | | | | | | | |
| 409017 | 65°00.884′, 50°12.644′ | 12.144 | 13.606 | 31.846 | | 11.917 | 13.544 | 31.582 |
| 409018 | 65°00.92′, 50°12.61′ | 12.137 | 13.507 | 31.976 | | 11.794 | 13.449 | 31.618 |
| 409022 | 65°01.532′, 50°13.343′ | 12.484 | 13.735 | 32.292 | | 12.047 | 13.583 | 31.861 |
| 409023 | 65°01.532′, 50°13.343′ | 13.682 | 13.864 | 34.088 | | 12.224 | 13.575 | 32.395 |
| 409025 | 65°01.01′, 50°12.65′ | 13.488 | 14.026 | 33.241 | | 12.438 | 13.806 | 32.082 |
| 409026 | 65°01.03′, 50°12.64′ | 13.337 | 13.864 | 34.094 | HF-leach | 18.608 | 15.597 | 32.813 |
| 409026 | | | | | HCl-leach | 16.564 | 15.033 | 33.302 |
| 409031 | 65°01.28′, 50°13.00′ | 12.030 | 13.305 | 31.565 | | 11.477 | 13.214 | 31.382 |
| Concordant granitoid sheets inamphibolites | | | | | | | | |
| 409019 | 65°01.80′, 50°13.77′ | 16.367 | 14.908 | 37.323 | | 13.088 | 14.113 | 32.448 |
| 409030 | 65°01.40′, 50°13.23′ | 17.419 | 15.000 | 37.595 | | 13.165 | 14.066 | 32.030 |

ondary isochrons by the fact that their slopes define apparent ages (of no geological significance whatsoever, but see Tera 2000) between 4.24 and 4.48 Ga well in excess of plausible intrusion ages. Rather, the slope of these secondary isochrons is determined by the relative timing of rock formation and feldspar recrystallisation (a process explained in detail by Rosholt et al. 1973).

Secondary feldspar-isochrons are a feature of the combined $^{235}U$–$^{207}Pb$ and $^{238}U$–$^{206}Pb$ systems, and occur because of the ability of feldspar to recrystallise with the Pb-isotopic composition of its host whole rock but without incorporating U, thus creating a snapshot of a particular point in Pb-isotopic evolution. If feldspars record the isotopic composition of a set of consanguineous, isochronous host rocks at some time between rock formation and today, like in our examples, the slope defined in common Pb-isotope space yields an apparent age much in excess of the rock formation age. For a comprehensive discussion of secondary feldspar-isochrons the reader is referred to the excellent treatment of this subject by Rosholt et al. (1973; pp. 989–991).

In the case of our SOI tonalite gneiss feldspar regression line (which will henceforth be called a secondary 'isochron', where the inverted commas indicate that statistically these regressions are errorchrons), the slope is 0.585, which, if erroneously interpreted as an age,

**Table 4** Pb-isotope data for Uivak and Nanokg neisses. These data were obtained by K.D.C. at the University of California (Santa Cruz). We retrospectively normalised the ratios to the recommended NBSSRM 981 values of Todt et al. (1996). Internal precision of all measurements was better than the standard reproducibility at Santa Cruz (that is, 0.16, 0.24 and0.41%). In contrast to the new SOI gneiss feldspars, these samples were only leached in weak nitric acid, resulting in less-reproducible duplicates

| Sample | $^{206}Pb/^{204}Pb$ | $^{207}Pb/^{204}Pb$ | $^{208}Pb/^{204}Pb$ | Sample | $^{206}Pb/^{204}Pb$ | $^{207}Pb/^{204}Pb$ | $^{208}Pb/^{204}Pb$ |
|---|---|---|---|---|---|---|---|
| 3.73-Ga Uivak gneiss whole rocks | | | | Nanok gneiss whole rocks continued | | | |
| KC-78–629A | 14.075 | 14.420 | 34.624 | KC-91–34A | 17.312 | 14.889 | 40.251 |
| KC-78–623C | 13.793 | 14.009 | 35.374 | KC-91–34B | 14.933 | 14.424 | 38.831 |
| KC-78–627B | 13.408 | 14.079 | 38.547 | KC-91–35A | 15.516 | 14.690 | 36.589 |
| 3.73-Ga Uivak gneiss feldspars | | | | KC-91–35B | 14.650 | 14.413 | 35.634 |
| KC-78–630A | 13.017 | 14.190 | 34.397 | KC-91–35H | 13.672 | 14.224 | 34.664 |
| Duplicate | 13.241 | 14.290 | 34.672 | KC-91–48B | 15.037 | 14.411 | 37.094 |
| KC-78–620D | 12.554 | 13.832 | 32.653 | KC-91–56B | 13.800 | 14.278 | 34.766 |
| KC-78–629A | 13.323 | 14.313 | 33.832 | KC-91–56G | 13.500 | 14.147 | 34.200 |
| KC-78–623C | 12.335 | 13.722 | 32.471 | Nanok gneiss feldspars | | | |
| Duplicate | 12.478 | 13.791 | 32.799 | KC-91–25A | 14.152 | 14.727 | 32.819 |
| KC-78–627B | 12.519 | 13.840 | 32.885 | Duplicate | 14.213 | 14.711 | 32.821 |
| Duplicate | 12.718 | 13.992 | 33.222 | KC-91–33A | 12.812 | 13.999 | 32.753 |
| KC-78–633D | 12.878 | 13.998 | 33.287 | Duplicate | 12.922 | 14.056 | 33.181 |
| Nanok gneiss whole rocks | | | | KC-91–35B | 12.867 | 14.077 | 32.678 |
| KC-91–25A | 15.215 | 14.440 | 40.287 | Duplicate | 12.902 | 14.109 | 32.891 |
| KC-91–33A | 15.154 | 14.393 | 40.220 | KC-91–56G | 12.673 | 13.971 | 32.258 |
| KC-91–33C | 15.076 | 14.452 | 37.044 | Duplicate | 12.716 | 14.000 | 32.513 |

would yield $4{,}480 \pm 77$ Ma (MSWD = 6,746). In the simplest case, a secondary feldspar-isochron is formed during a single (metamorphic) Pb-isotope homogenisation event at ($t_h$) from a suite of consanguineous samples. Provided that the magmatic age ($t_m$) of the suite is known, $t_h$ can be calculated from the slope of the isochron. The combinations of rock formation ages and feldspar recrystallisation times that yield a slope of 0.585 are illustrated in Fig. 6A. Because all the SOI gneisses for which zircon has been studied in detail have a simple U-Pb age distribution and because the zircons have a simple structure, we assume that the magmatic protoliths formed at 3.82 Ga. The SOI TTG secondary feldspar-'isochron' then constrains the age of feldspar crystallisation to 1.95 Ga (Fig. 6A). The secondary feldspar-'isochron' minimum and maximum ages of 4,394 and 4,560 Ma translate into homogenisation at 1,808 and 2,216 Ma, respectively. The SOI gneisses and the coastal gneisses of northern Labrador clearly experienced a complex tectonic and metamorphic history which the simple interpretation of the secondary feldspar-'isochron' model does not reproduce. However, there are three features of the secondary 'isochron' that we believe justify the simple two-stage treatment for the purpose of Pb-isotope interpretation.

First, provided that the U/Pb ratio of the whole rock is not greatly disturbed in the course of Pb-isotope homogenisation of previous events, a valid secondary isochron can form during the last event of homogenisation. We recall that the whole-rock regression age, although scattered and imprecise, is still within error of the much more precise U-Pb zircon ages. This suggests that while the scatter does document a certain disturbance of the whole-rock U/Pb ratios, the general U-Pb isotopic integrity of the SOI TTG gneisses has remained preserved. Hence, although the secondary feldspar-'isochron' that is now preserved may only be the latest in a whole succession, its slope still contains valid information about $t_m$, $t_h$ and initial isotope composition.

Second, both in the IGB area and in northern Labrador there is evidence for Palaeoproterozoic isotope resetting. While there is no doubt that the strongest metamorphic overprints in both areas occurred at ca. 3.6 Ga and again between 2.6 and 2.7 Ga (e.g. Collerson 1983b; Baadsgaard et al. 1986), the important point for the secondary feldspar-'isochron' is that several studies have found reset mineral chronometers that require low-grade metamorphism or recrystallisation long after 2.6 Ga. Pankhurst et al. (1973) showed that K-Ar, Ar-Ar and Rb-Sr mica and amphibole ages from Itsaq gneiss samples were all reset and that a late Archaean and a Proterozoic (1.6–1.7 Ga) homogenisation event were recorded. Essentially identical early to mid-Proterozoic apparent ages were obtained by Baadsgaard et al. (1976) in their K-Ar, Rb-Sr and U-Pb mineral isotope study of the coastal Itsaq gneisses. In the IGB area, Baadsgaard (1983) found that discordant U-Pb sphene and apatite dates were unable to pin-point the exact date of secondary metamorphism in the range of 1,500–2,800 Ma. In a later study, Baadsgaard et al. (1986) documented two separate Sr-isotope resetting events in the IGB area at 2,550 and $1{,}623 \pm 65$ Ma, the latter within the limited resolution of $t_h$ calculated from our secondary feldspar-'isochron'. In northern Labrador, there is strong evidence from homogenisation of Sr-isotope systematics in the Uivak gneisses that the last pervasive Sr-isotope homogenisation occurred at ca. 1,800 Ma. Collerson (1983b) discovered that individually cut compositional layers from two slabbed Uivak gneisses yielded secondary 'isochrons' with regression ages of 1,798 and 1,884 Ma, while the total rock sample still aligned along early Archaean reference lines. This

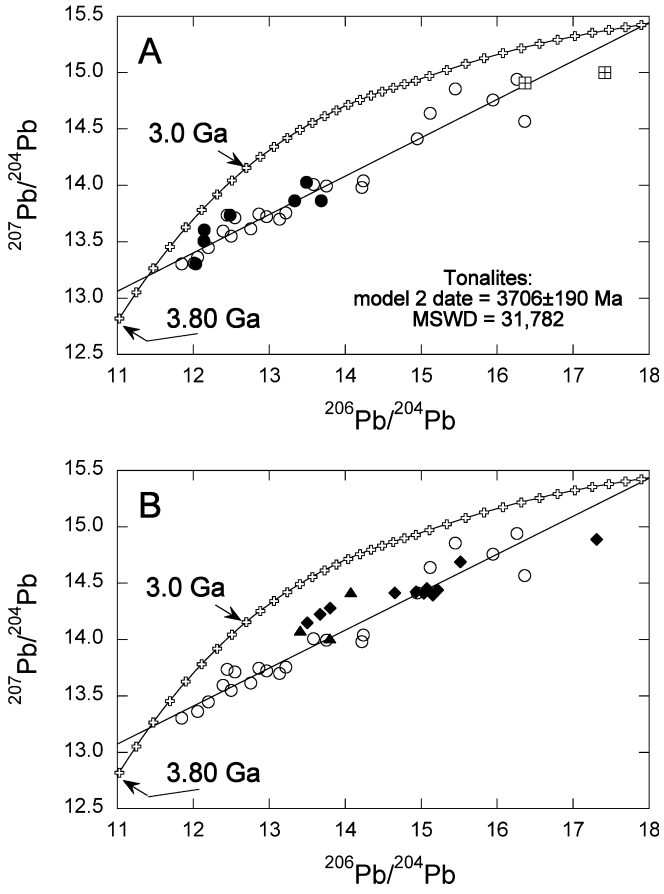


**Fig. 4** Common Pb diagrams for whole-rock data. **A** Whole-rock data (Table 3) shown separately for the SOI tonalite gneisses (*open circles*), amphibolite gneisses (*solid circles*) and layer-parallel granite melts (*crossed squares*). Regression line is shown for tonalite gneisses only. The mantle evolution line (*solid fine curve connecting open crosses*) is that of Kramers and Tolstikhin (1997). Distance between *crosses* corresponds to a 100-Ma time step. **B** Labrador whole-rock data (Table 4) shown separately for Nanok gneisses (*solid diamonds*) and Uivak gneisses (*solid triangles*) compared to SOI tonalite gneisses (*open circles*). Regression lines and mantle model as in **A**

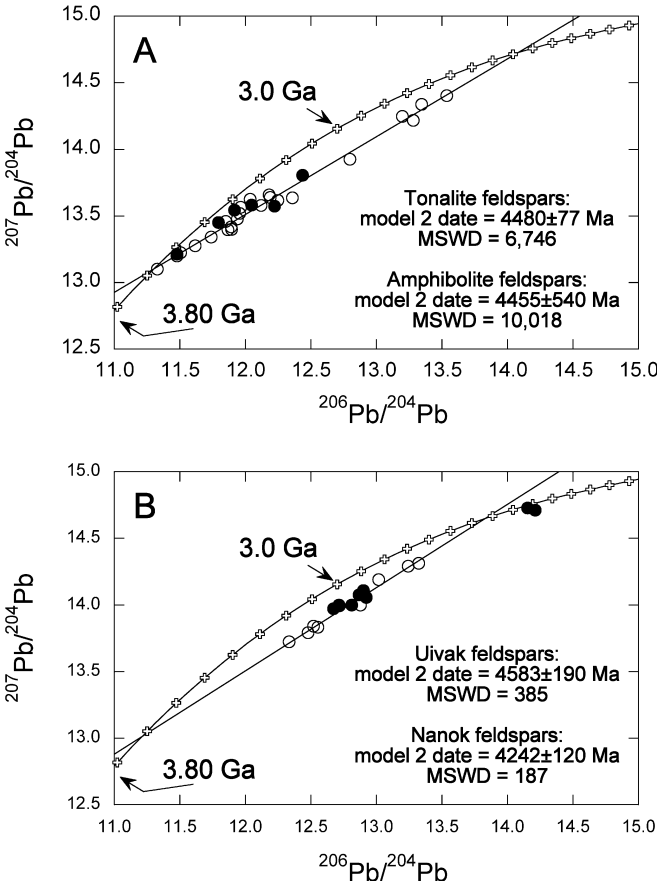


**Fig. 5** Common Pb diagrams for feldspar data. **A** Feldspar data (Table 3) plotted separately for SOI tonalite (*open circles*) and amphibolite gneisses (*solid circles*). Regression line is shown for tonalite gneisses only. Mantle evolution line as in Fig. 4. **B** Labrador data (Table 4) shown separately for Uivak gneisses (*open circles*) and Nanok gneisses (*solid circles*). Regression line shown is for Uivak data only

indicates that the Rb-Sr system was reopened at the centimeter-scale during Proterozoic events that affected the North Atlantic craton (Collerson 1983b).

Third, 'homogenisation' in the context of feldspar Pb-isotopes refers to partial or complete exchange of Pb-isotopes between the whole rock and the feldspar, which could have occurred due to dynamic recrystallisation (all our plagioclase samples are recrystallised) or diffusional exchange in response to a thermal event. Limited isotope exchange between the whole rock and only some portions of the feldspar still yields a valid slope (Fig. 6B) for simple systems that experienced only one isotope resetting. In other words, while the whole-rock-feldspar 2-point dates of partially homogenised feldspars will be older than $t_h$ (like in our example, where they range between 2,700 and 3,500 Ma), the slope of the secondary feldspar-'isochron' remains valid. In more complex situations with multiple feldspar recrystallisations, partial homogenisation will introduce scatter into the isochron. The SOI gneiss secondary feldspar-'isochron' shows scatter outside the reproducibility that can be expected for the leaching protocol. This was estimated from the Pb-isotope ratios of one plagioclase (409010) that plots farthest from the secondary isochron. Its $^{206}Pb/^{204}Pb$, $^{207}Pb/^{204}Pb$ and $^{208}Pb/^{204}Pb$ ratios were reproduced to within 0.2, 0.02 and 0.02% in two separate leaching experiments (see Table 3). The much larger scatter between samples is therefore not due to inefficient leaching of labile Pb but was caused by incomplete homogenisation or by superimposed effects of several homogenisation events.

In brief, the slope of the observed secondary feldspar-'isochron' reflects isotopic exchange between feldspar and whole rock during one or more metamorphic events, the latest of which occurred during the mid-Proterozoic.

## Pb-isotope heterogeneity in the early Archaean

The main purpose of feldspar and ore Pb-isotope studies is not geochronological but to address whether analysed

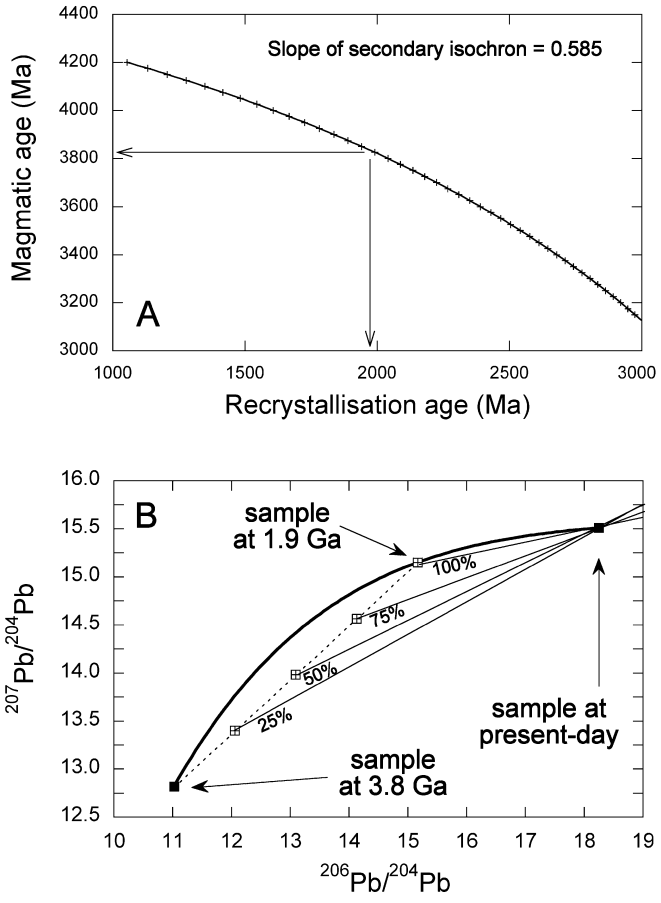


**Fig. 6 A** Combinations of magmatic ages and recrystallisation ages that yield a constant secondary isochron slope of 0.585, i.e. corresponding to an apparent age of 4,471 Ma. Because of the gentle curvature, relatively small changes in magmatic age require larger shifts in recrystallisation age. *Arrows* indicate likely magmatic age of SOI tonalite gneisses and corresponding recrystallisation age of ca. 1,950 Ma. **B** Effect of partial feldspar-whole-rock homogenisation on 2-point 'ages' and slope of secondary feldspar-isochron. Shown is a calculated evolution curve (*bold*) for a 3.80-Ga-old rock (with $\mu = 9$) to the present day. In the case of complete homogenisation with the whole rock at 1.90 Ga, feldspar (*open crossed square*) plots along the evolution curve and the 2-point slope (*solid fine line*) with the present-day whole rock corresponds to the 1.90-Ga age of homogenisation. Partial homogenisation (three examples shown, corresponding to 25, 50 and 75% mixtures), however, produces less radiogenic feldspar Pb-isotope compositions that yield meaningless 2-point 'ages' (3,042, 3,447 and 3,664 Ga) with the whole rock. The important point is that all feldspar datapoints (fully and partially homogenised) still plot on the correct secondary isochron (*stippled line*)

samples show evidence for U/Th/Pb fractionation of their sources and, if so, to explore implications for terrestrial differentiation. In this regard, the Pb/Pb system has the advantage that in the early Earth's silicate reservoirs both $^{206}Pb/^{204}Pb$ and $^{207}Pb/^{204}Pb$ increased by several percent per 100 Ma, the latter especially benefiting from the much higher $^{235}U$ abundance at that time. Therefore, differentiation in the early Earth is expected to have left a record in initial isotope ratios recorded by samples with very low $\mu$, such as feldspars, ores and chemical sediments. In order to compare the initial Pb-isotope composition of different early Archaean rock types from SW Greenland and northern Labrador, it is necessary to refer to modelled evolution curves. The loci of these evolution lines reflect the rate of radiogenic ingrowth in particular terrestrial reservoirs. As such they depend on model assumptions which can be verified by comparing observed with modelled isotope composition.

There are two basic approaches to model Pb-isotope evolution curves. The first is to define a time series of input data to which a model curve is fitted by adjusting the $\mu$ of the reservoir in a series of successive 'stages'. This concept is widely applied to other radiogenic isotope systems, most notably Sm-Nd, where the isotope evolution of the 'depleted' mantle is defined by data from the most radiogenic basaltic rocks at any given time. Because of the mobility of U it is impossible to derive *bona fide* initial Pb-isotope ratios for ancient basaltic rocks, so that original attempts at modelling 'terrestrial' Pb-isotope evolution (naturally referring to the silicate Earth only) used data for U-free ores as input parameters. However, it was soon realised (e.g. Kanasewich 1968) that there exist strong isotopic variabilities between ores of the same age, indicating that Pb in those ores was derived from sources that had experienced evolution with different $\mu$ (and Th/U). Due to the degree of isotopic variability in ores and feldspars, illustrated in Fig. 1, it is necessary to make significant and equivocal assumptions regarding the origin of the Pb. Once the extent of variability in ore Pb-isotope ratios became appreciated [for a thorough discussion see Hofmann (2001)], distinction between 'conformable' and 'anomalous' was no longer warranted, so that most recent attempts at devising Pb-isotope evolution curves have used a less data-dependent approach.

The most widely known example of this second class of models was developed by Stacey and Kramers (1975). Rather than fitting an evolution line to a time-series of input data, this model was largely constrained by the following input values: the age of the Earth; the initial isotope composition of the Earth (as approximated by meteoritic troilite); and the Pb-isotope composition of present-day 'accessible' Earth. The latter parameter was estimated by measurements of MORB and pelagic sediments. As such, the Stacey and Kramers (1975) model provided only a single evolution curve which averages the various silicate Earth reservoirs and does not do justice to the fact that the ore and feldspar database (Fig. 1) demonstrates existence of strongly fractionated (in terms of U and Pb) reservoirs in the distant geological past.

More elaborate kinds of this type of model (e.g. Zartman and Haines 1988) have since addressed this problem and have proposed evolution curves for several crustal and mantle silicate Earth reservoirs. The evolution lines of 'old upper continental crust' and 'young lower continental crust' of Kramers and Tolstikhin's (1997) model encompass much of the variability seen in initial Pb-isotopes preserved in ores and feldspars

(Fig. 1). Recalling that the continental crust harbours more than a third of the terrestrial U and Th, it is clear that its extraction from and recycling back into the mantle have had the strongest effect on the present-day isotope composition of the MORB-source mantle. In contrast to the Sm-Nd system, which is relatively insensitive to extraction and isolation of large volumes of early Archaean crust (e.g. Nägler and Kramers 1998), the present-day differences in Pb-isotopes between MORB and average upper crust (as approximated by sediment) provide a strong control over the continental crust volume vs. time curve. In particular, this difference, combined with the average crustal Nd-isotope mantle derivation age of 2–2.5 Ga, implies that continental crust volume was small in the early Archaean and that the strongest net growth of the continents occurred between 3 and 2 Ga. Independent geochemical evidence supports the S-shape of the continental crust volume vs. time curve (e.g. Collerson and Kamber 1999).

However, these advances in plumbotectonics are of limited relevance to the interpretation of Pb-isotopes of the earliest Archaean samples (i.e. $>3.5$ Ga). The reason for this is that most models (understandably) did not attempt to derive evolution lines for the primordial terrestrial crust that existed prior to formation and preservation of continental crust s.s. The model of Kramers and Tolstikhin (1997) does use a transient protocrust, whose Pb-isotope evolution, however, was not modelled. Rather, the protocrust in their model is fully recycled into the mantle at 4.3 Ga and its Pb-isotope evolution was not considered important for any preserved terrestrial samples. However, in the past few years, an increasing number of $>3.8$-Ga zircons have been reported and the known terrestrial record now dates back to 4.4 Ga (Wilde et al. 2001), indicating that evolved rocks existed in the terrestrial protocrust. Kramers (2001) speculated that an enriched early crust that persisted for several 100 Ma might be the reason for the large variability in early Archaean $^{207}Pb/^{204}Pb$ ratios. Here we test how far our new Pb-isotope data for early Archaean samples are compatible with this proposal.

Our discussion is based on a comparison between data from the earliest accessible Earth and the MORB-source mantle evolution line of the Kramers and Tolstikhin (1997) model. Reference to a model facilitates comparison and construction of specific evolution curves. Because we are primarily interested in exploring the extent of early Archaean Pb-isotope heterogeneity it is not relevant whether the model MORB-source evolution line is correct. The locus of the model curve between 4.3 and 3.6 Ga is largely determined by increase in bulk silicate Earth $\mu$ as a function of metal and sulphide segregation into the core. If the prototerrestrial material had a substantially higher $\mu$ (e.g. 6–8) than carbonaceous chondrites, similar to the range inferred for ordinary chondrites, core formation would not have had a strong effect on silicate Earth Pb-isotope evolution and the MORB-source would have plotted at higher $^{207}Pb/^{206}Pb$ than that modelled by Kramers and Tolstikhin (1997). We will discuss this possibility in more detail later, but will initially focus on describing the extent of observed Pb-isotope heterogeneity.

There are five independent observations regarding the Pb-isotope systematics of the early Archaean Earth:

1. First, feldspars from the Godthaabsfjord 3.65-Ga Amîtsoq gneisses, belonging to a relatively late and well-developed intrusive pulse (McGregor 2000), contain the least radiogenic silicate Pb known on Earth. This plots very close to the Kramers and Tolstikhin (1997) MORB-source curve at ca. 3.66 Ga (Fig. 7A). The 3.65-Ga age for the magmatic protoliths of these gneisses is well established from U-Pb zircon dating (e.g. Nutman et al. 1996; Whitehouse et al. 1999). They also yield 3.65-Ga whole-rock regression dates in the Pb-Pb, Rb-Sr and Sm-Nd systems (Kamber and Moorbath 1998). The combined whole-rock and feldspar Pb-Pb regression line intersects the Kramers and Tolstikhin (1997) MORB-source evolution at 3.66 Ga (Fig. 7A).
2. Second, the very high $^{207}Pb/^{206}Pb$ ratio of IGB BIF. Moorbath et al.'s (1973) BIF regression line yields the same 3.7-Ga age as Nutman et al. (1997), obtained by U-Pb zircon dating of a number of IGB metasediments. However, the regression line intersects the MORB-source evolution line at an impossibly young 'age' of 3.38 Ga (Fig. 7B). This observation prompted Moorbath et al. (1973) to postulate an immediate precursor to BIF that experienced a very different U/Pb history from the mantle. More recently, Kamber et al. (2001) have extended that discussion to IGB siliceous carbonates which indicate derivation of Pb from a similarly high-$\mu$ source (Fig. 7B).
3. Third, the position of IGB galena Pb-isotope ratios relative to the MORB-source curve (Fig. 7B). With the exception of galenas from one locality, they all plot to the left of the mantle evolution lines and presently define the least radiogenic terrestrial Pb known. This is not an artefact of inaccurate mass discrimination correction, as Frei and Rosing (2001) have demonstrated excellent reproducibility between data obtained on thermal and ICP mass spectrometers. Frei and Rosing (2001) regarded the offset between all IGB galena data and mantle evolution lines as significant and concluded that this required an elevated $\mu$ for the source of those galenas.
4. The SOI TTG secondary feldspar-'isochron' intersects the mantle evolution curve at unexpectedly radiogenic values, corresponding to a nominal date of 3.69 Ma, instead of the expected 3.81 Ga (Fig. 5a). The difference in $^{207}Pb/^{204}Pb$ between 3.69 and 3.81 Ga is very substantial and well outside the regression accuracy. However, if the linear feldspar array was formed in multiple events of incomplete homogenisation, it may have experienced some clockwise rotation, resulting in artificially 'young' intersection with the mantle evolution curve. However, there is no obvious bias in the regression line

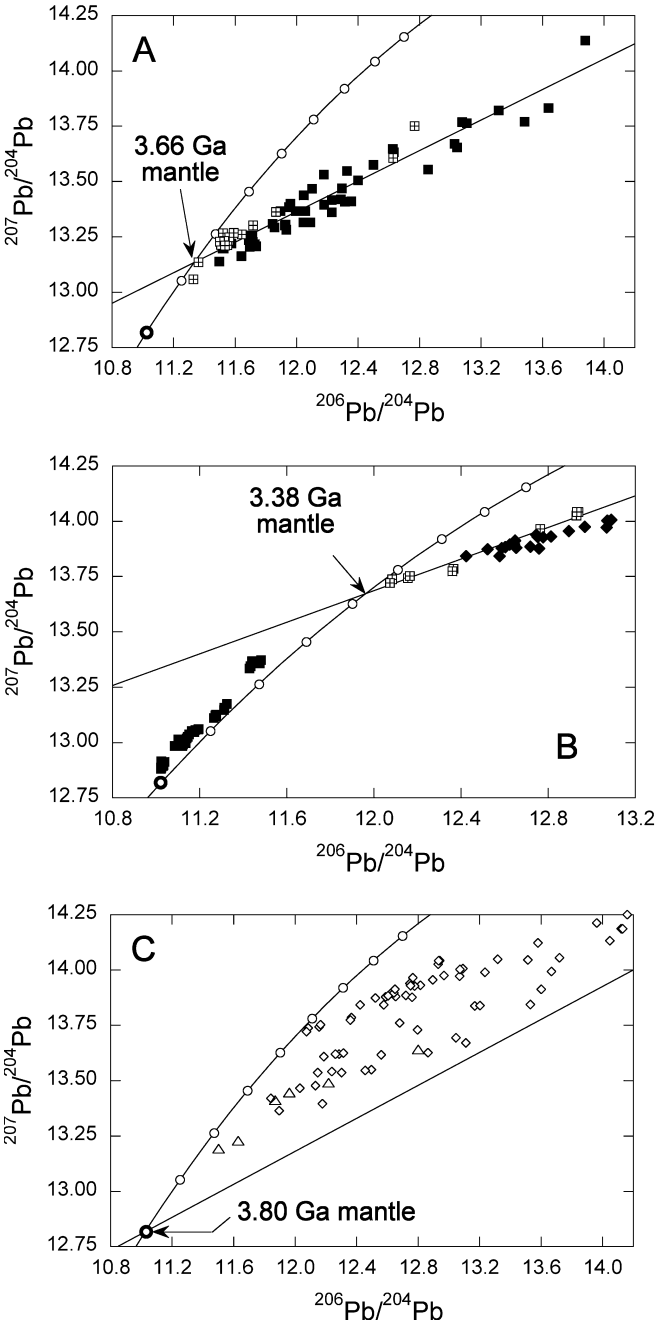


**Fig. 7** Pb-isotope variability in early Archaean lithologies expressed relative to the MORB-source mantle evolution curve of Kramers and Tolstikhin (1997), of which 100-Ma steps are plotted as *open circles* (the 3.8-Ga point is highlighted as a *larger circle with bold stroke*). **A** 3.65-Ga Godthaabsfjord Amîtsoq gneisses define a whole-rock (*solid squares*) and feldspar (*open crossed squares*) regression line that intersects the modelled evolution line at 3.66 Ga. Feldspar data points plot very close to the 3.7- to 3.6-Ga section of the curve. **B** IGB galena data (*solid squares*; see Table 1) plot significantly to the left of the model curve (with four exceptions, which were omitted for clarity), while BIF data points (*open crossed squares*) measured by Moorbath et al. (1973) plot along a 3.7-Ga regression line that intersects the evolution line at 3.38 Ga. Other possible chemical sediments [*solid diamond symbols*; data from Kamber et al. (2001)] also plot along the BIF regression line. **C** A 3.80-Ga isochron starting from coeval mantle composition plots significantly below the isotope composition of all IGB supracrustals [*open diamonds*; data from Table 1; Moorbath et al. (1973); Kamber et al. (2001)] and Akilia enclave metamorphic rocks [*open triangles*; data from Kamber and Moorbath (1998)]

(Fig. 5a), which is defined equally well by the most and least radiogenic datapoints. This argues against systematic rotation. Furthermore, the whole-rock regression age, which is within error of the expected age of the rocks, also intersects the mantle evolution curve at an improbably young date of 3.63 Ga.

5. The Uivak feldspar regression line intersects the mantle evolution curve at 3.72 Ga (Fig. 5b), very similar to the U-Pb zircon age of 3.73 Ga.

In summary, two of the five lithologies (Amîtsoq and Uivak gneisses) have Pb-isotope systematics that are formally consistent with derivation from the mantle source modelled by Kramers and Tolstikhin (1997), while three types of lithologies (galena, chemical sediments and SOI gneisses) point to source areas that experienced a stage of significantly higher U/Pb evolution than the modelled mantle evolution line. In the following section we discuss the possible significance of this finding.

## Model Pb-isotope evolution of high-$\mu$ source

The challenge of interpreting the observed early Archaean Pb-isotope heterogeneity is to identify the nature of the sources (i.e. crust vs. mantle) and to estimate the time of source separation necessary to generate the observed isotope variability. There are several possible scenarios which are encompassed by two end-member models. The first end-member assumes that the samples that require a source with a relatively low time-integrated U/Pb ratio were derived from a depleted portion of the mantle, while those that project to high initial $^{207}Pb/^{204}Pb$ ratios were derived from an undepleted or even enriched mantle domain. By contrast, the second end-member assumes that the mantle was not differentiated (i.e. neither depleted nor enriched) and that samples with radiogenic initial $^{207}Pb/^{204}Pb$ ratios were derived from a crustal source. There are three observations that favour the latter model. We discuss these observations before we describe the parameters for our preferred second end-member scenario.

1. Because the bulk Earth $\mu$ is unknown and because terrestrial core formation could have been completed within 35 Ma (Schoenberg et al. 2002a), there is a possibility that the mantle evolution line to which we have compared the early Archaean data could plot at too low $^{207}Pb/^{204}Pb$ ratios at a given $^{206}Pb/^{204}Pb$ ratio. This is because in Kramers and Tolstikhin's (1997) model the $\mu$ of the silicate Earth gradually increased as Pb was removed with metal into the core. If, however, the core formed very rapidly, the period of retarded Pb-isotope evolution would have been

shorter, resulting in a mantle evolution line that plots at higher $^{207}Pb/^{204}Pb$ ratios. The most extreme case assumes a constant single-stage $\mu$ evolution, which corresponds to a bulk silicate Earth where core formation had no influence on Pb-isotope evolution. Indeed, a single-stage (4,568-Ma) mantle with a $\mu$ of 8.25 (Fig. 8A) plots significantly above the MORB-source mantle evolution line of Kramers and Tolstikhin (1997) and projects to the $^{207}Pb/^{204}Pb$ independently estimated for bulk silicate Earth by Galer and Goldstein (1996) and Kamber and Collerson (1999). However, as shown in the inset of Fig. 8A the IGB galena datapoints do not plot at sufficiently high $^{207}Pb/^{204}Pb$ to be derived from such an undepleted mantle source. If the $\mu$ of the single-stage model is adjusted to a value of 7.8, to yield a closer fit with the galena data (inset Fig. 8B), it becomes evident that such a mantle source would contain insufficient U to explain the present-day silicate Earth (i.e. the present-day composition of this source plots at lower $^{207}Pb/^{204}Pb$ than modern MORB; Fig. 8B). Furthermore, the single-stage mantle source fails to provide a solution to the IGB BIF data in that the BIF regression line intersects at too young an 'age' (inset Fig. 8B). In brief, the IGB galena data do not seem to outline a single-stage mantle evolution curve (such as could be expected for bulk silicate Earth).

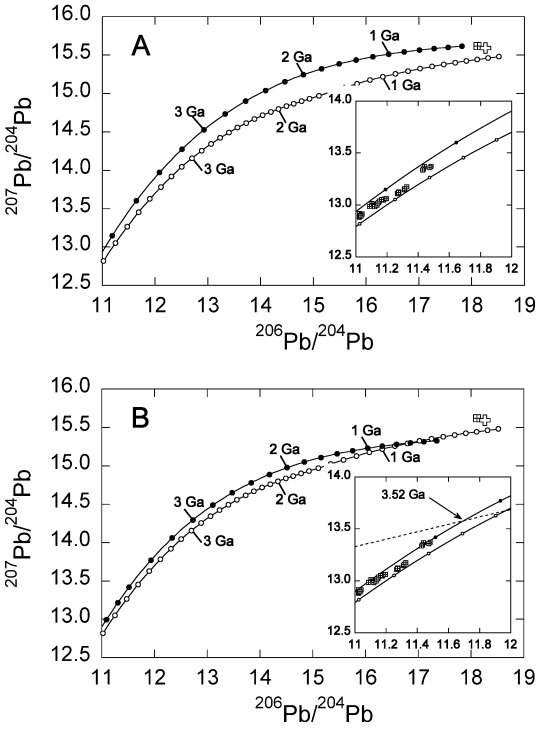


**Fig. 8** Comparison of mantle evolution lines. **A** The MORB-source mantle evolution line (*open circles*) of Kramers and Tolstikhin (1997) plots well below a single-stage evolution with a constant $\mu$ of 8.25 (*solid circles*) that projects to the present-day Pb-isotope composition estimates of bulk silicate Earth: *crossed open square* by Galer and Goldstein (1996); *open large cross* by Kamber and Collerson (1999). *Inset* shows that the IGB galena (*small crossed open squares*) plot between both lines. **B** Similar comparison but showing a single-stage evolution (*solid circles*) with a lower $\mu$ of 7.8 to yield a closer fit to the IGB galena data (see *inset*). Note mismatch with present-day bulk silicate Earth estimates (*main graph*) and intercept with IGB BIF regression line (*stippled line* in *inset*) at 3.52 Ga

2. The second argument in favour of a crustal nature for the high-$\mu$ source is the observation that this source is most apparent in metasediments, and particularly chemical metasediments, while the lower-$\mu$ source is seen in the voluminous TTG gneisses (Godthaabsfjord Amîtsoq and Uivak). Indeed, the highest $^{207}Pb/^{204}Pb$ ratios are found in IGB BIF and siliceous dolomites (Fig. 7B), which strongly implies a surface origin of the Pb that records derivation from a high-$\mu$ environment. Importantly, metapelites from the IGB also plot at considerably higher initial $^{207}Pb/^{204}Pb$ than contemporaneous mantle (Fig. 7C), lending support to the hypothesis that they represent erosion products of ancient terrestrial crust that may have persisted (and weathered) for several 100 Ma prior to deposition as clastic sediments. It is in these rocks that Schoenberg et al. (2002b) recently discovered $^{182}W$-deficits, which they linked to accumulation of meteoritic W (from the heavy bombardment period) transported from weathered impact debris. Remelting of pre-existing high-$\mu$ crust could explain existence of TTG gneisses with high initial $^{207}Pb/^{204}Pb$.
3. The third supporting argument is based on initial zircon Hf-isotope ratios from ancient zircons which, until recently, were interpreted to indicate derivation of the original melt from a strictly chondritic to mildly depleted reservoir. However, new experimental (Nir-El and Lavi 1998) and geological recalibrations (Scherer et al. 2001) of the $^{176}Lu$ decay constant fundamentally change this interpretation because of a significant shift in the chondrite reference Hf-isotope evolution. Amelin et al. (2000) and Scherer et al. (2001) noted that if the new $^{176}Lu$ decay constant is correct, initial Hf-isotopes recorded by early Archaean zircons would imply existence of an enriched reservoir. In order to evolve to the observed Hf-isotope compositions by ca. 4.0 Ga, this reservoir would have had to separate from convecting mantle at least 4.3 Ga ago (Scherer et al. 2001). The most likely candidate for the proposed enriched reservoir is a terrestrial protocrust.

For these reasons we believe that the initial Pb-isotope variability seen in early Archaean rocks is best discussed in terms of existence of a terrestrial protocrust. This explanation is further supported by the fact that, unlike with mantle evolution lines, a single crustal model can be derived that provides an acceptable fit to all observations.

The difference in required $\mu$ between a sample source and contemporaneous mantle is a function of the source's separation age. The longer the source spent in isolation from the convecting (model) mantle, the

smaller the difference in $\mu$. For example, the 3.71-Ga IGB BIF source could have been isolated at 4.2 Ga and evolved with a $\mu$ of 13.8. Alternatively, if source separation occurred only at 3.80 Ga, a $\mu$ of 41 is required (Kamber et al. 2001). Similarly, the SOI tonalite gneiss source could have separated at 4.3 Ga and evolved with such a moderately high $\mu$ of 10.5, or it could have separated 200 Ma later with a $\mu$ of 12.5. In this manner, an infinite number of possible sources could be postulated for each available data set. However, the important observation is that one single model can be derived that provides acceptable fits to all observations. The evolution line of this high-$\mu$ Pb source is outlined by the galena datapoints, which define a curved array subparallel to the mantle evolution line (Fig. 9A). In order for a source to plot at significantly higher $^{207}Pb/^{204}Pb$ ratios than the mantle at a given $^{206}Pb/^{204}Pb$, without rapidly diverging from a parallel trajectory, a very early mantle separation (e.g. 4.3 Ga) with a moderately high $\mu$ is required. Later source separation (e.g. 4.1 Ga) with such a moderately high $\mu$ cannot explain the galena datapoints that plot farthest to the left of the mantle evolution line (Fig. 9B). The galena data therefore require an early source separation (Frei and Rosing 2001) for which we propose 4.3 Ga. An identical separation age for an enriched source was postulated by Scherer et al. (2001) in their reinterpretation of Hf-isotope ratios recorded by single early Archaean zircons. Slightly older (post-Moon formation) separation ages provide similar fits to the Pb data, but the quality of fit deteriorates rapidly for younger separation ages. For a 4.3-Ga source separation, the best fit to the combined galena, tonalite and BIF data was found with a source $\mu$ of 10.5. This describes a trajectory that encompasses all but the four most extreme galena compositions (Fig. 9B). It yields a model age of 3.86 Ga for the SOI tonalite gneiss secondary feldspar-'isochron' (which is easily within error of the slope of that regression line), and a 3.70-Ga model age for the 3.71-Ga IGB BIF (Fig. 9C). Importantly, Pb-isotope compositions (Table 1) of all other typical IGB lithologies are also perfectly compatible with this model, as they extrapolate to intersections between 3.82 and 3.70 Ga, which is exactly the range found in zircon U-Pb ages (Nutman et al. 1997), Sm-Nd (Kamber et al. 1998) and Lu-Hf regressions [Villa et al. (2001); recalculated from data by Blichert-Toft et al. (1999)].

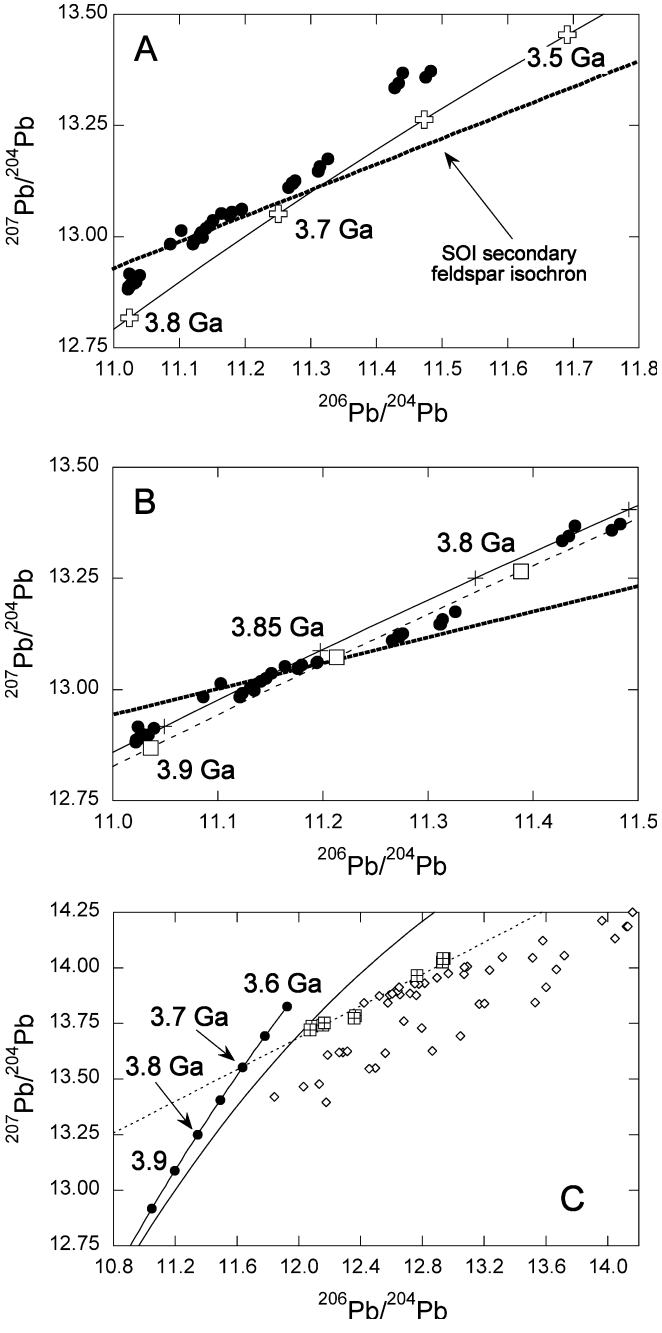


**Fig. 9** Pb-isotope evolution model. **A** Comparison between IGB galena data (*solid circles*; data sources as in Fig. 1) and mantle evolution model (*solid line connecting open crosses*) of Kramers and Tolstikhin (1997). The SOI tonalite secondary feldspar-'isochron' intersects the mantle model at ca. 3,680 Ma, which is at least 120 Ma younger than the magmatic age. The extent of mismatch in mantle model age is best appreciated by comparison with the model mantle composition at 3.80 Ga. The secondary 'isochron' projects directly into a prominent cluster of galena data. **B** Comparison of two source models for the SOI tonalite gneisses. The first (*broken line connecting open squares*) was calculated assuming a mantle separation age of 4.1 Ga and a $\mu$ of 12.5. It was modelled to intersect the secondary feldspar-'isochron' at 3.85 Ga but fails to explain the Pb-isotope compositions of all but the least anomalous galenas. A mantle separation age of 4.3 Ga with a $\mu$ of 10.5 (*solid line connecting + symbols*) results in a much better match with the galena data. It intersects the secondary feldspar-'isochron' at 3.87 Ga, which is within error of the resolution of the 'isochron's slope. **C** Comparison between mantle evolution line (*solid curve, no symbols*) with the 4.3-Ga, $\mu = 10.5$ model (*solid line connecting small solid circles*, spaced at 50-Ma intervals) derived in **B**. It can be seen that the Pb-isotope compositions of all IGB lithologies (*open diamonds*) project to between 3.70 and 3.82 Ga along appropriate reference isochrons (stippled isochron corresponds to 3.70 Ga). The 3.70-Ga BIF isochron (*stippled line connecting crossed squares*) of Moorbath et al. (1973) projects exactly to 3.70 Ga on the model source

There is some scatter in the galena data (Fig. 9B), which probably exceeds analytical uncertainty. The spread of ratios *along* the model evolution line is easily explained as reflecting ore sources ranging in age from 3.75 to 3.91 Ga. This explanation differs from that of Appel et al. (1978) and Richards and Appel (1987) who attributed the variation in Pb-isotope ratios of galenas, which they regarded as late Archaean in age, to reflect slight differences in $\mu$ of a single ancient Pb source of a common age. Note, however, that Richards and Appel (1987) worked on a much smaller data array, which did not clearly define the sub-parallel character relative to the mantle curve. We prefer to interpret the variation in galena Pb-isotope ratios as largely reflecting differences in age of the Pb source rocks, allowing for the possibility that mineralisation occurred at 3.70 Ga (Frei et al. 1999). There is a large cluster of galenas whose model ages of ca. 3.86 Ga (Fig. 9B) exceed the age of the oldest known lithologies in the IGB. The SOI tonalite gneiss secondary feldspar-'isochron' projects into that data cluster, which indicates that the ore could have been derived by later remobilisation of Pb from feldspar in TTG similar to SOI. Figure 2 illustrates that the SOI gneisses are exposed in close proximity (0–30 km to the south) of the IGB. Furthermore, possibly detrital zircon grains from proposed IGB quartzites and from a paragneiss from the southern IGB cluster at exactly that age (Nutman et al. 1997; Nutman 2001). Zircon U-Pb dates of ca. 3.86 Ga have also been reported from Labrador, both from inherited xenocrysts of some Uivak gneisses (Collerson 1983a; Schiøtte et al. 1989) and from portions of detrital zircons in Nulliak quartzites (Nutman and Collerson 1991; Nutman 2001). The oldest U-Pb zircon dates from the North Atlantic craton date back to 3,897 and 3,910 Ma and are found in proposed IGB metasediments and Nanok gneisses (Collerson 1983a ; Nutman et al. 1997), implying the existence of evolved crustal rocks of that age. In our model the magmatic hosts of these zircons were the source of the least radiogenic known terrestrial Pb, which is now stored in the IGB galenas with a 3.91-Ga model age. The deviation of some galena datapoints towards the right of the high-$\mu$ source (Fig. 9B) is explained by (minor) admixture of juvenile mantle source material. In summary, the Pb-isotope systematics of all IGB and SOI lithologies can be explained with a local source that separated from the mantle ca. 4.3 Ga ago and evolved with a $\mu$ of ca. 10.5.

## Discussion

In the following discussion we follow the recent (informal) convention of defining Hadean as $>4.0$ Ga, but we emphasise that preservation of 3.8- to 4.0-Ga rocks is equally important and may hold the clues to preservation of even older Hadean isotopic memory.

### Implications for early differentiation

The key observation regarding claims for the existence of radiogenic isotope heterogeneity within the early Archaean silicate Earth is the requirement for long-term (i.e. 300- to 500-Ma) source isolation. Differences in radiogenic isotope ratios recorded in earliest Archaean rocks (e.g. ca. 3.8 Ga) therefore require formation and isolation of enriched or depleted reservoirs in Hadean time. Here we postulate that Pb-isotope evolution of the early Archaean segment of the North Atlantic craton is explained by the early terrestrial upper mantle boundary layer model of Campbell and Griffiths (1993).

The mean age of oceanic lithosphere is presently ca. 60 Ma and models of oceanic crust production rate indicate that it may have been even shorter in the past. It is therefore impossible to create isotopic anomalies of the magnitude seen in studied lithologies over the lifetime of even the oldest known oceanic lithosphere (ca. 200 Ma) prior to subduction. However, as pointed out by Campbell and Griffiths (1993), in the absence of the subduction mechanism, a thick, relatively buoyant basaltic shell may have encased the mantle and survived for up to 500 Ma. Heat loss by conduction through stable basaltic lithosphere forms a cool, unstable, depleted boundary layer at the base of the crust. After 100–200 Ma, this mantle material cools to the point where it forms a cold plume (Campbell and Griffiths 1992), which sinks into the deep mantle with little entrainment of ambient mantle. Campbell and Griffiths (1993) commented on the possibility that this process could provide a means by which depleted mantle material was transported to the core-mantle boundary, from where it could be entrained into hot plumes (and brought back to the surface) at a much later stage. Here we stress the fact that the same process of cold plumes provides the early mantle with an inherent mechanism by which the most depleted material was removed from the uppermost mantle. In other words, in complete contrast to the present situation, it is more likely that isotope anomalies persisted in Hadean basaltic crust than in the upper mantle and that these crustal anomalies are 'enriched' in character.

Accepting the hypothesis of a stable Hadean basaltic crust for the terrestrial planets (e.g. Choblet and Sotin 2001), we now describe the geotectonic framework of the Pb-isotope evolution model for the early North Atlantic craton. The first step of this model involves creation of a thick basaltic crust at ca. 4.3 Ga with a $\mu$ of ca. 10.5. This represents an increase in $\mu$ by 26% from the coeval mantle value of 8.34 (Kramers and Tolstikhin 1997), which appears reasonable in view of the higher incompatibility of U. Importantly, because of the relatively low Pb concentration in MORB-like basalt [$\leq$ 0.5 ppm on average; Jochum and Verma (1996)], creation of a thick global basaltic crust would not greatly affect the Pb-isotope evolution of the complementary depleted mantle. If the Hadean basaltic shell resembled enriched lunar basalts, which also have an elevated $\mu$ (Nyquist and Shih 1992), there is a possibility of significant complementary deple-

tion in the mantle. However, because of the aforementioned gravitational instability of the uppermost cooled mantle material, portions of the depleted residue would likely have sunk into the deepest mantle and been replaced by primitive mantle. We envisage that the basaltic protocrust differentiated, by episodic remelting, to more silicic compositions. This could have occurred in response to exposure of the crustal base to convecting asthenosphere, immediately following departure of a cold plume. Melting of hydrated amphibolite, if present in the mafic protocrust, could have produced silicic rocks of tonalitic or monzodioritic composition (e.g. Nutman et al. 1999). The oldest evidence in the IGB for differentiation is preserved as 3.90-Ga zircon (Nutman et al. 1997) and, if our model is correct, ca. 3.91-Ga-old source rocks for galena (Fig. 9B). Zircon evidence from the Acasta gneisses (Bowring and Williams 1999) and from Western Australia (e.g. Wilde et al. 2001) points to even earlier differentiation in these areas.

However, our model of a stable basaltic Hadean shell explicitly refutes operation of processes such as sediment recycling or melting in subduction zones. We therefore regard the interpretation of highly variable O-isotope ratios in Hadean zircons in terms of crustal assimilation or melting of greywacke protoliths at 4.3–4.4 Ga (Mojzsis et al. 2001; Wilde et al. 2001) as too speculative to question the fundamental constraints imposed by terrestrial cooling. The collection of recovered fragments from the Moon, which is patently depleted in water and volatiles, contains a considerable variety of evolved rocks, such as granites, granophyre and quartz-monzodiorites, some of which contain zircons (Nyquist and Shih 1992). Zircon U-Pb dates from these evolved rocks are in the range 4.37–3.90 Ga, but mostly fall in the older parts of this range (Meyer et al. 1996). The quoted authors conclude that the formation of lunar granite was not restricted to a single episode in lunar history, as, for example, during final solidification of the magma ocean. Rather, it appears to be the result of localised differentiation of individual plutons that intruded into the lunar crust or eventually erupted as felsic lavas.

In the IGB and SOI, differentiation, erosion and transformation of magmatic precursors into sediments proceeded at rapid pace between 3.90 and 3.80 Ga, but intrusion of the most voluminous TTGs, both in Greenland and Labrador, only started after 3.80 and peaked at 3.73 Ga (Labrador) and 3.65 Ga (Greenland). We view the creation of these granitoids as marking the initiation of subduction and rapid recycling of the Hadean basaltic shell (a process that may have been aided by the late heavy bombardment with meteorites).

Most importantly, both the 3.73-Ga Uivak gneisses and the most voluminous and dominant 3.65-Ga pulse of Amîtsoq gneisses have Pb-isotope characteristics of the convecting mantle, and not of the high-$\mu$ Hadean basalt shell (Figs. 5B and 10A, respectively). This could imply a change in magma source from remelting the Hadean high-$\mu$ basalt shell to melting of the early Archaean convecting mantle. This view is supported by concordant Rb-Sr and Sm-Nd regression lines for the Uivak and Godthaabsfjord TTG gneisses, which both yield intercepts corresponding to isotope ratios of contemporaneous, slightly depleted mantle (Collerson 1983a; Moorbath et al. 1997). The Pb-isotope characteristics of the oldest parts of the North Atlantic craton are thus testimony to the advent of subduction and provide a rare glimpse of Hadean differentiation.

## Implications for Godthaabsfjord TTG gneiss Pb-isotope evolution

The co-existence of two reservoirs, from ca. 4.3 to ca. 3.65 Ga, with appreciably different $\mu$ (i.e. the high-$\mu$ Hadean basaltic crust and the mildly depleted mantle), complicates interpretation of Pb-isotope ratios of *individual* samples. This is best illustrated with the 3.65 Godthaabsfjord TTG gneiss whole-rock regression line (Fig. 10A). This intersects the depleted mantle evolution line at 3.66 Ga, which is the agreed age based on U-Pb zircon dating (e.g. McGregor 2000), and on the slope of the regression line itself. The intersection with the Hadean basaltic crust evolution line, however, is found at 3.85 Ga, because of faster evolution due to a higher source $\mu$. Individual whole-rock datapoints that plot along the regression line cannot, therefore, be unambiguously assigned to the 3.65-Ga sample suite or to potentially older generations of TTGs (such as the SOI tonalite gneisses). The only incontrovertible direct Pb-isotope evidence for a ≥3.8-Ga age of some of those samples would be a feldspar Pb-isotope composition that plots to the left of the mantle evolution line (akin to IGB galena). To date, such compositions have not been found (e.g. Kamber and Moorbath 1998). Indirect evidence against an age greater than 3.65 Ga for the samples studied by Kamber and Moorbath (1998) is provided by a comparison between feldspar and whole-rock data. In the case of the samples studied by Kamber and Moorbath (1998) and Gancarz and Wasserburg (1977), feldspar data, including the most radiogenic data points, plot closely along the 3.65-Ga whole-rock regression line (Fig. 10A). In the 3.80- to 3.82-Ga SOI tonalite gneisses, however, the feldspar Pb-isotope data define their own, much steeper trend (Fig. 10A), which we interpret as a secondary 'isochron'. Because such a trend is not seen in the Godthaabsfjord TTG gneiss data and because of the very low U-contents of igneous zircons, we argue that the very unradiogenic Pb of these samples is an original magmatic feature (Kamber and Moorbath 1998). However, we cannot exclude the possibility that a few of the whole-rock data points are from samples that are older than 3.65 Ga.

## Implications for preservation of ≥3.8-Ga rocks and minerals

Despite the fact that the early Earth, at least by 4.0 Ga, must have been covered by crust (probably basaltic),

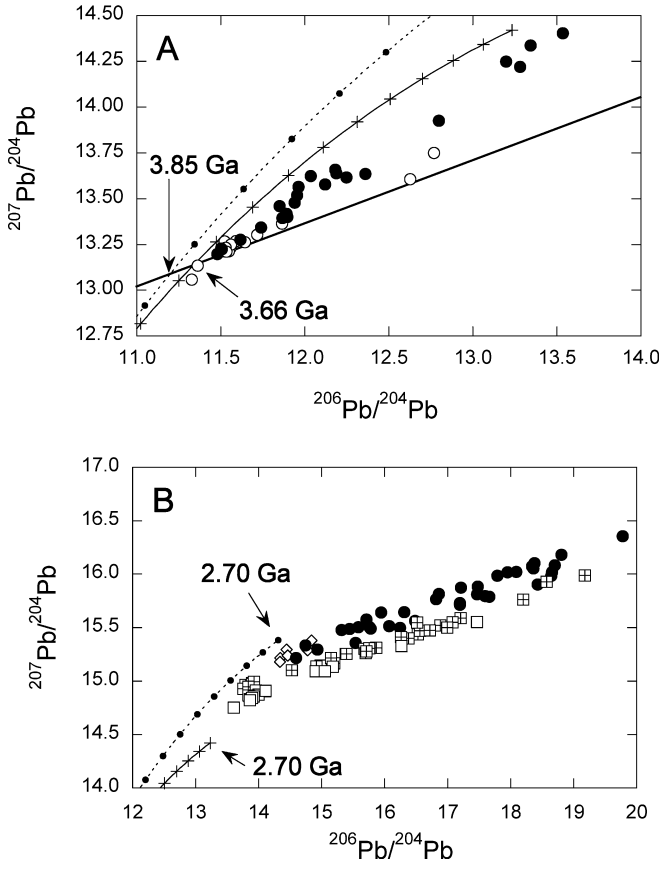


**Fig. 10** Common Pb diagrams. **A** Intersection of 3.65-Ga Godthaabsfjord TTG gneiss regression line (*bold solid*; after Kamber and Moorbath 1998) with the depleted mantle curve (*solid fine line connecting + symbols*) of Kramers and Tolstikhin (1997) is at 3.66 Ga, while an intersection is found at 3.85 Ga with the Hadean basaltic crust evolution (*stippled line connecting small solid circles*). All leached plagioclase data points (*open circles*) compiled and presented by Kamber and Moorbath (1998) also plot along the 3.65-Ga regression line. This contrasts with the plagioclase data points for the SOI TTG gneisses (*solid circles*), which define their own, distinctively steeper trend. **B** Comparison of late Archaean model Pb-isotope compositions with data from late Archaean granitoid intrusions from high-$\mu$ cratons. *Solid line connecting (+) symbols* is depleted mantle curve by Kramers and Tolstikhin (1997) and *stippled line connecting small solid circles* is Hadean basaltic crust evolution derived in this study. Both evolution lines are shown to 2.70 Ga. Importantly, the least radiogenic datapoints of 2.6 to 2.73-Ga granitoids (typically from leached feldspars) from all cratons plot closely along a mixing line (not shown) connecting the depleted mantle evolution with that of the Hadean basaltic crust. The granitoids that plot closer to the 2.7-Ga Hadean basaltic crust evolution display a higher proportion of preserved Hadean crust in their source. *Symbols* and data sources for granitoids are: *solid circles* (Zimbabwe craton, northernmost Limpopo belt; Berger and Rollinson 1997); *open diamonds* (western Slave craton, Point Lake area; Davis et al. (1996); *crossed squares* (Wyoming craton, Beartooth Mountains; Wooden and Mueller 1988); and *open squares* (Yilgarn craton, Murchison province; Wang et al. 1993)

there is very limited direct evidence of its existence. The terrestrial situation contrasts with that of the Moon (almost complete preservation of ≥3.8-Ga crust) and of Mars, where resurfacing did lead to appreciable denudation and reworking of ancient highlands (Hynek and Phillips 2001). The scarcity of ≥3.8-Ga material on Earth is a consequence of poor preservation. This implies tectonic instability and almost complete recycling of early crust. In the framework of an Earth encased with a relatively static basaltic shell (Campbell and Griffiths 1993), the disappearance of ≥3.8-Ga crust is explained by the onset of subduction. Because the early basaltic shell was not created along subduction zones it lacked the buoyant lithospheric mantle keel, which is the key feature for survival of modern continental crust. Furthermore, in a plate tectonic framework, crust can only persist on a lithospheric mantle keel, it follows that only those fragments of early crust could survive that developed a keel *immediately* after onset of a tectonic framework driven by subduction. In other words, those portions of the early crust that experienced rapid addition of voluminous continental material (i.e. TTGs, granites and basalts) were also equipped with a complementary lithospheric mantle keel, which ultimately saved them from subduction. This conclusion appears to be supported by the geology of the other two major areas that preserve significant ≥3.8-Ga material.

Bowring et al. (1989a), Bowring and Housh (1995), Stern and Bleeker (1998) and Bowring and Williams (1999) have reported U-Pb zircon dates of 3.8–4.03 Ga from the Acasta gneisses of the Slave craton (Northwest Territories, Canada). This provides strong evidence for existence of chemically evolved protoliths, which subsequently experienced a complex geological history. Importantly, the >3.8-Ga Acasta gneisses are surrounded by younger gneisses, with zircon dates between 3.6 and 3.8 Ga, identical to the situation in the North Atlantic craton. Geological events at 3.75 and 3.60 Ga can also be inferred from the complex U-Pb date patterns of those zircons that contain portions exceeding 3.8 Ga in age.

The oldest known terrestrial material by far (up to 4.4 Ga) are detrital zircons preserved in mid-Archaean metasedimentary rocks in the northwestern corner of the Yilgarn craton of Western Australia (Froude et al. 1983; Mojzsis et al. 2001; Wilde et al. 2001). The metasediments are tectonically juxtaposed against orthogneisses with interpreted magmatic ages between 3,730 and 3,380 Ma. The oldest in-situ rocks are represented by the 3,680-Ma Meeberrie gneiss and the 3,730-Ma layered intrusion of the Manfred complex. Detrital zircons of 3.5–3.75 Ga are also abundant in the Mt Narryer quartzite [see Fig. 2 of Kinny et al. (1990)], pointing to the former existence of significant components of early Archaean crust in the basement. Thus, the Mt Narryer gneiss complex contains the 3.75- to 3.60-Ga orthogneisses that we regard as crucial for preservation of ≥3.8-Ga material.

There is only very limited further evidence for preserved ≥3.8-Ga material. Dodson et al. (1988) reported 3.81-Ga U-Pb dates for detrital zircons from the Zimbabwe craton, which also contains 3.6-Ga granitoids in the Towke area (e.g. Taylor et al. 1991). Mueller et al.

(1992) discovered 3.96-Ga detrital zircons in quartzites of the Wyoming province, where the oldest known trondhjemitic gneisses date back to 3.5 Ga (Mueller et al. 1996). Although evidence for coupled occurrence of $>3.8$-Ga material and 3.6- to 3.75-Ga TTG magmatism is incomplete, we stress, as our final conclusion, the observation that all the mentioned gneiss terrains occur on so-called high-$\mu$ cratons, as discussed below.

### The high-$\mu$ signature as a remnant of Hadean basaltic crust

It has long been known that some (Archaean) cratons have a so-called high-$\mu$ Pb-isotope signature (e.g. Oversby 1975), while others (such as the Pilbara or Kaapvaal cratons) appear to have been derived from material with mantle-like U/Pb evolution. In the original definition, high-$\mu$ cratons are those that contain rocks whose initial Pb-isotope compositions require evolution in a source with a higher $\mu$ than MORB-source mantle. This does not necessarily imply that the rocks themselves inherit a high $\mu$ from the source. There is no agreed classification of cratons according to source $\mu$, and we restrict our discussion here to the following examples: the Slave craton (e.g. Bowring et al. 1989b); the Yilgarn craton (e.g. Fletcher et al. 1988); the Zimbabwe craton (Taylor et al. 1991); the Wyoming province (Wooden and Mueller 1988); and the North Atlantic craton (despite its very unradiogenic present-day isotope composition). Explanations for the high-$\mu$ character of those cratons have favoured either sediment recycling or intra-crustal differentiation of U from Pb (e.g. Kramers and Tolstikhin 1997). Both explanations require the upper crust to assume a higher $\mu$ than the lower crust. In the sediment subduction model, sedimentary Pb of high-$\mu$ character (and ancient unradiogenic Nd) is cycled through arcs and ultimately reappears in the upper crust as arc magmas (Mueller and Wooden 1988). In the intracrustal differentiation model, U, Th and Pb are fractionated in the course of magmatic differentiation. High-$\mu$ Pb in such models is preserved by preferential erosion of juvenile material.

On the premise that the coexistence of $>3.8$-Ga material, 3.6- to 3.75-Ga TTGs and a general high-$\mu$ character is not fortuitous, we propose a new model in which the high-$\mu$ character of the aforementioned cratons could be inherited from Hadean basaltic crust. We notice the good fit (Fig. 10B) between the modelled 4.3-Ga basaltic crust evolution line ($\mu = 10.5$) and initial isotope ratios from these cratons. The high-$\mu$ character of these cratons is well expressed in voluminous mid- to late-Archaean granitoids, which invariably contain Nd-isotope ratios indicative of a long crustal pre-history (e.g. Berger and Rollinson 1997). Furthermore, there is Os-isotope evidence from the Zimbabwe craton for initiation of growth of subcontinental lithospheric mantle at 3.8 Ga (Nägler et al. 1997).

We envisage that some Hadean high-$\mu$ basaltic crust and its differentiation products (such as the SOI gneisses and the source rocks of $>3.8$-Ga zircons) were preserved in the emerging mantle-derived TTG-bearing cratonic nuclei which started forming along the earliest terrestrial subduction zones between 3.75 and 3.60 Ga. The rationale for this hypothesis is that widespread subduction-related magmatism between 3.75 and 3.60 Ga would have created a sufficiently deep subcontinental lithospheric mantle keel to stabilise the cratonic nuclei against destructive convectional forces. The basaltic high-$\mu$ rocks that were incorporated into the cratonic nuclei formed part of the source of later Archaean magmatism and, in that sense, the high-$\mu$ signature of these mid- to late-Archaean rocks may be hinting to the extreme antiquity of their source. Whether Hadean basaltic (and more differentiated) crust is properly preserved on Earth is still unknown, but the earliest pulses of non-mantle-derived orthogneisses (e.g. SOI, Nanok) are the most promising areas to harbour them.

## Summary

Steep feldspar Pb-isotope arrays, which if interpreted as single-stage 'isochrons' yield apparent Hadean ages, are compatible with U-Pb zircon age evidence for an age of 3.80–3.82 Ga of SOI TTG gneisses in Greenland and an age of 3.81–3.92 Ga of the Nanok gneisses in northern Labrador. We interpret these arrays as secondary 'isochrons', which formed during feldspar-whole-rock isotope homogenisation, which last occurred in a 1.8- to 2.2-Ga tectonometamorphic event. The feldspar secondary isochrons are the first, albeit indirect, Pb-isotope evidence from terrestrial silicate samples for in-situ rocks older than 3.65 Ga.

Comparison of the secondary feldspar-isochrons with initial Pb-isotope information from metasediments and galena from the IGB and a combined feldspar-whole-rock regression line from the coastal 3.65-Ga Amîtsoq gneisses demonstrates that Pb-isotope variability (mainly in $^{207}Pb/^{204}Pb$) existed in the early Archaean. Neither the magmatic precursors of the ≥3.80-Ga TTG gneisses nor the metasediments or the galena in the IGB were derived from the mantle because they do not plot along trajectories that project to the Pb-isotope composition of present-day bulk silicate Earth. They require the existence of a terrestrial reservoir with a higher U/Pb ratio than mantle. Significantly, a single high-$\mu$ source that separated from the mantle at ca. 4.3 Ga with a $\mu$ of ca. 10.5 provides a good fit to all these observations. We propose that this source was the Hadean (basaltic?) crust which, in the absence of the subduction process, encased the early Earth. Differentiation of the early high-$\mu$ basaltic crust could have occurred in response to gravitational sinking of cold mantle material (Campbell and Griffiths 1992) or meteorite impact, and produced zircon-bearing magmatic rocks. The subchondritic

Hf-isotope ratios of ≥3.8-Ga zircons support this model (Amelin et al. 2000) provided that the redetermined $^{176}$Lu decay constant of Scherer et al. (2001) is correct. Our model of a stable basaltic Hadean shell explicitly refutes operation of processes such as sediment recycling or melting of hydrated material in subduction zones [as recently suggested by Mojzsis et al. (2001) and Wilde et al. (2001)]. Instead, we propose that initiation of terrestrial subduction occurred at ca. 3.75 Ga, at which stage most of the Hadean basaltic shell (and its differentiation products) was recycled into the mantle, because of the lack of a stabilising mantle lithosphere. Therefore, the preservation of ≥3.8-Ga terrestrial rocks and minerals is not fortuitous, but reflects intrusion of voluminous granitoids immediately after establishment of global subduction because of complementary creation of a lithospheric keel.

Finally, we note that preservation of ≥3.8-Ga terrestrial material (in-situ rocks and zircons) globally appears to be restricted to cratons with a high-$\mu$ source character (North Atlantic, Slave, Zimbabwe, Yilgarn and Wyoming). Although most of the direct early Archaean memory of these cratons was erased in later geological events, we suggest that their high-$\mu$ signature is an ancient isotopic memory pointing to the extreme antiquity of the source of these crustal domains and that the Pb-isotope systematics of these provinces are ultimately explained by reworking of material that was derived from Hadean basaltic crust.

**Acknowledgements** We thank Robert Frei and Minik Rosing for sending us a preprint of their galena paper, and R. Zartman, L. Neymark and Y. Amelin for very thorough reviews. A. Hofmann's editorial interest is greatly appreciated. B.S.K. acknowledges financial support from the Deputy Vice-Chancellor at UQ. The UQ MC-ICPMS was purchased with partial support from an ARC equipment grant to K.D.C. M.J.W. acknowledges the support of the Swedish Natural Sciences Research Council (grant S-650–19981611/2000). The research councils of Denmark, Finland, Norway and Sweden jointly support the NordSIMS facility. Research in northern Labrador was supported by US NSF and Canadian NSERC grants to K.D.C. S.M. and M.J.W. collected the Greenland samples under the auspices of the Isua Multidisciplinary Research Project, and thank P.W.U. Appel for logistic support. This is a contribution to the Isua Multidisciplinary Research Project and NordSIMS contribution number 69.

## References

Amelin Y, Lee DC, Halliday AN (2000) Early–middle Archaean crustal evolution deduced from Lu-Hf and U-Pb isotopic studies of single zircon grains. Geochim Cosmochim Acta 64:4205–4225

Appel PWU, Moorbath S, Taylor PN (1978) Least radiogenic terrestrial lead from Isua, West Greenland. Nature 272:524–526

Baadsgaard H (1983) U-Pb isotope systematics on minerals from the gneiss complex at Isukasia, West Greenland. Rapp Gronlands Geol Unders 125:48–51

Baadsgaard H, Lambert RS, Krupicka J (1976) Mineral isotopic age relationships in the polymetamorphic Amîtsoq gneisses, Godthaab District, West Greenland. Geochim Cosmochim Acta 40:513–527

Baadsgaard H, Nutman AP, Rosing M, Bridgwater D, Longstaffe FJ (1986) Alteration and metamorphism of Amîtsoq gneisses from the Isukasia area, West Greenland: recommendations for isotope studies of the early crust. Geochim Cosmochim Acta 50:2165–2172

Berger M, Rollinson H (1997) Isotopic and geochemical evidence for crust-mantle interaction during late Archaean crustal growth. Geochim Cosmochim Acta 61:4809–4829

Black LP, Gale NH, Moorbath S, Pankhurst RJ, McGregor VR (1971) Isotopic dating of the very early Precambrian amphibolite gneisses from the Godthaab District, West Greenland. Earth Planet Sci Lett 12:245–259

Blichert-Toft J, Albarède F, Rosing M, Frei R, Bridgwater D (1999) The Nd and Hf isotopic evolution of the mantle through the Archean. Results from the Isua supracrustals, West Greenland, and from the Birimian terranes of West Africa. Geochim Cosmochim Acta 63:3901–3914

Bodet F, Schärer U (2001) Pb isotope systematics and time-integrated Th/U of SE-Asian continental crust recorded by single K-feldspar grains in large rivers. Chem Geol 177:265–285

Bowring SA, Housh T (1995) The Earth's early evolution. Science 269:1535–1540

Bowring SA, Williams IS (1999) Priscoan (4.00–4.03 Ga) orthogneisses from northwestern Canada. Contrib Mineral Petrol 134:3–16

Bowring SA, Williams IS, Compston W (1989a) 3.96 Ga gneisses from the Slave province, Northwest Territories, Canada. Geology 17:971–975

Bowring SA, King JE, Housh TB, Isachsen CE, Podosek FA (1989b) Neodymium and lead isotope evidence for enriched early Archaean crust in North America. Nature 340:222–225

Campbell IH, Griffiths RW (1992) The changing nature of mantle hotspots through time—implications for the chemical evolution of the mantle. J Geol 100:497–523

Campbell IH, Griffiths RW (1993) The evolution of the mantle's chemical-structure. Lithos 30:389–399

Cheong CS, Kwon ST, Sagong H (2002) Geochemical and Sr-Nd-Pb isotopic investigation of Triassic granitoids and basement rocks in the northern Gyeongsang Basin, Korea: implications for the young basement in the East Asian continental margin. Island Arc 11:25–44

Choblet G, Sotin C (2001) Early transient cooling of Mars. Geophys Res Lett 28:3035–3038

Collerson KD (1983a) Ion probe zircon geochronology of the Uivak gneisses: implications for the evolution of the early terrestrial crust in the North Atlantic craton. In: Ashwal LD, Card KD (eds) Proc Worksh of a cross section of Archaean Crust. LPI Tech Rep 83–03, Houston, pp 28–33

Collerson KD (1983b) The Archaean gneiss complex of northern Labrador. 2. Mineral ages, secondary isochrons, and diffusion of strontium during polymetamorphism of the Uivak gneisses. Can J Earth Sci 20:707–718

Collerson KD, Kamber BS (1999) Evolution of the continents and the atmosphere inferred from Th-U-Nb systematics of the depleted mantle. Science 283:1519–1522

Collerson KD, McCulloch MT, Nutman AP (1989) Sr and Nd-isotope systematics of polymetamorphic Archean gneisses from southern West Greenland and northern Labrador. Can J Earth Sci 26:446–466

Collerson KD, Kamber BS, Schoenberg R (2002) Applications of accurate, high-precision Pb isotope ratio measurements by multi-collector ICP-MS. Chem Geol 188:65–83

Davis WJ, Gariepy C, van Breemen O (1996) Pb isotopic composition of late Archaean granites and the extent of recycling early Archaean crust in the Slave Province, northwest Canada. Chem Geol 130:255–269

De SK, Chacko T, Creaser RA, Muehlenbachs K (2000) Geochemical and Nd-Pb-O isotope systematics of granites from the Taltson Magmatic Zone, NE Alberta: implications for early Proterozoic tectonics in western Laurentia. Precambrian Res 102:221–249

Dodson MH, Compston W, Williams IS, Wilson JF (1988) A search for ancient detrital zircons in Zimbabwean sediments. J Geol Soc Lond 145:977–983

Fedo CM, Myers JS, Appel PWU (2001) Depositional setting and paleogeographic implications of Earth's oldest supracrustal rocks, the >3.7 Ga Isua Greenstone belt, West Greenland. Sediment Geol 141:61–77

Fletcher IR, Rosman KJR, Libby WG (1988) Sm-Nd, Pb-Pb and Rb-Sr geochronology of the Manfred Complex, Mount Narryer, Western Australia. Precambrian Res 38:343–354

Frei R, Rosing MT (2001) The least radiogenic terrestrial leads: implications for the early Archaean crustal evolution and hydrothermal-metasomatic processes in the Isua Supracrustal Belt (West Greenland). Chem Geol 181:47–66

Frei R, Bridgwater D, Rosing M, Stecher O (1999) Controversial Pb-Pb and Sm-Nd isotope results in the early Archean Isua (West Greenland) oxide iron formation: preservation of primary signatures versus secondary disturbances. Geochim Cosmochim Acta 63:473–488

Froude CF, Ireland TR, Kinny PD, Williams IS, Compston W, Williams IR, Myers JS (1983) Ion-microprobe identification of 4100–4200 Myr old terrestrial zircons. Nature 304:616–618

Galer SJG, Goldstein SL (1996) Influence of accretion on lead in the Earth. In: Basu A, Hart S (eds) Earth processes: reading the isotopic code. American Geophysical Union, Washington, DC, pp 75–98

Gancarz AJ, Wasserburg GJ (1977) Initial Pb of the Amîtsoq gneiss, West Greenland, and implications for the age of the Earth. Geochim Cosmochim Acta 41:1283–1301

Goldstein SJ, Jacobsen SB (1987) The Nd and Sr isotopic systematics of river-water dissolved material: implications for the sources of Nd and Sr in seawater. Chem Geol 66:245–272

Hemming SR, McDaniel DK, McLennan SM, Hanson GN (1996) Pb isotope constraints on the provenance and diagenesis of detrital feldspars from the Sudbury Basin, Canada. Earth Planet Sci Lett 142:501–512

Hemming SR, Gwiazda RH, Andrews JT, Broecker WS, Jennings AE, Onstott TC (2000) $^{40}Ar/^{39}Ar$ and Pb-Pb study of individual hornblende and feldspar grains from southeastern Baffin Island glacial sediments: implications for the provenance of the Heinrich layers. Can J Earth Sci 37:879–890

Hofmann AW (2001) Lead isotopes and the age of the Earth: a geochemical accident. In: Lewis CLE, Knell SJ (eds) The age of the Earth: from 4004 BC to AD 2002. Geol Soc Spec Lond, Publ 190, pp 223–236

Hynek BM, Phillips RJ (2001) Evidence for extensive denudation of the Martian highlands. Geology 29:407–410

Jochum KP, Verma SP (1996) Extreme enrichment of Sb, Tl and other trace elements in altered MORB. Chem Geol 130:289–299

Kamber BS, Collerson KD (1999) Origin of ocean-island basalts: a new model based on lead and helium isotope systematics. J Geophys Res 104:25,479–25,491

Kamber BS, Moorbath S (1998) Initial Pb of the Amîtsoq gneiss revisited: implication for the timing of early Archaean crustal evolution in West Greenland. Chem Geol 150:19–41

Kamber BS, Moorbath S (2000) Initial Pb of the Amîtsoq gneiss revisited: implications for the timing of early Archaean crustal evolution in West Greenland—reply. Chem Geol 166:309–312

Kamber BS, Moorbath S, Whitehouse MJ (1998) Extreme Nd-isotope heterogeneity in the early Archaean—fact or fiction? Case histories from northern Canada and West Greenland—reply. Chem Geol 148:219–224

Kamber BS, Moorbath S, Whitehouse MJ (2001) The oldest rocks on Earth: time constraints and geological controversies. In: Lewis CLE, Knell SJ (eds) The age of the Earth: from 4004 BC to AD 2002. Geol Soc Spec Lond, Publ 190, pp 177–203

Kanasewich ER (1968) The interpretation of lead isotopes and their geological significance. In: Hamilton EI, Farquhar RM (eds) Radiometric dating for geologists. Wiley, London, pp 147–223

Kinny PD, Wijbrans JR, Froude DO, Williams IS, Compston W (1990) Age constraints on the geological evolution of the Narryer Gneiss Complex, Western-Australia. Aust J Earth Sci 37:51–69

Klötzli US, Koller F, Scharbert S, Höck V (2001) Cadomian lower-crustal contributions to Variscan granite petrogenesis (South Bohemian Pluton, Austria): constraints from zircon typology and geochronology, whole-rock, and feldspar Pb-Sr isotope systematics. J Petrol 42:1621–1642

Kramers JD (2001) The smile of the Cheshire cat. Science 293:619–620

Kramers JD, Tolstikhin IN (1997) Two terrestrial lead isotope paradoxes, forward transport modelling, core formation and the history of the continental crust. Chem Geol 139:75–110

Ludwig KR (1999) Isoplot/Ex rev. 2.49—a geochronological toolkit for Microsoft Excel. Berkeley Geochron Center Spec Publ 1a:1–52

McGregor VR (2000) Initial Pb of the Amîtsoq gneiss revisited: implications for the timing of early Archaean crustal evolution in West Greenland—comment. Chem Geol 166:301–308

Meyer C, Williams IS, Compston W (1996) Uranium-lead ages for lunar zircons: evidence for a prolonged period of granophyre formation from 4.32 to 3.88 Ga. Meteorit Planet Sci 31:370–387

Mojzsis SJ, Harrison TM, Pidgeon RT (2001) Oxygen-isotope evidence from ancient zircons for liquid water at the Earth's surface 4,300 Myr ago. Nature 409:178–181

Möller A, Mezger K, Schenk V (1998) Crustal age domains and the evolution of the continental crust in the Mozambique Belt of Tanzania: combined Sm-Nd, Rb-Sr, and Pb-Pb isotopic evidence. J Petrol 39:749–763

Moorbath S, O'Nions RK, Pankhurst RJ (1973) Early Archaean age for the Isua iron formation, West Greenland. Nature 245:138–139

Moorbath S, O'Nions RK, Pankhurst RJ (1975) The evolution of early Precambrian crustal rocks at Isua, West Greenland—geochemical and isotopic evidence. Earth Planet Sci Lett 27:229–239

Moorbath S, Whitehouse MJ, Kamber BS (1997) Extreme Nd-isotope heterogeneity in the early Archaean—fact or fiction? Case histories from northern Canada and West Greenland. Chem Geol 135:213–231

Mueller PA, Wooden JL (1988) Evidence for Archean subduction and crustal recycling, Wyoming province. Geology 16:871–874

Mueller PA, Wooden JL, Nutman AP (1992) 3.96 Ga zircons from an Archean quartzite, Beartooth Mountains, Montana. Geology 20:327–330

Mueller PA, Wooden JL, Mogk DW, Nutman AP, Williams IS (1996) Extended history of a 3.5 Ga trondhjemitic gneiss, Wyoming province, USA: evidence from U-Pb systematics in zircon. Precambrian Res 78:41–52

Myers JS (2001) Protoliths of the 3.8–3.7 Ga Isua greenstone belt, West Greenland. Precambrian Res 105:129–141

Nägler TF, Kramers JD (1998) Nd isotopic evolution of the upper mantle during the Precambrian: models, data and the uncertainty of both. Precambrian Res 91:233–252

Nägler TF, Kramers JD, Kamber BS, Frei R, Prendergast MDA (1997) Growth of subcontinental lithospheric mantle beneath Zimbabwe started ≥3.8 Ga: A Re-Os study on chromites. Geology 25:983–986

Neymark LA, Amelin Y, Larin AM (1994) Pb-Nd-Sr isotopic and geochemical constraints on the origin of the 1.54–1.56 Ga Salmi Rapakivi granite-anorthosite batholith (Karelia, Russia). Mineral Petrol 50:173–193

Nir-El Y, Lavi N (1998) Measurement of the half-life of $^{176}Lu$. Appl Radiat Isot 49:1653–1655

Nutman AP (2001) On the scarcity of >3900 Ma detrital zircons in ≥3500 Ma metasediments. Precambrian Res 105:93–114

Nutman AP, Collerson KD (1991) Very early Archaean crustal-accretion complexes preserved in the North Atlantic craton. Geology 19:791–794

Nutman AP, Allaart JH, Bridgwater D, Dimroth E, Rosing M (1984) Stratigraphic and geochemical evidence for the de-

positional environment of the early Archaean Isua supracrustal belt, southern West Greenland. Precambrian Res 25:365–396
Nutman AP, McGregor VR, Friend CRL, Bennett VC, Kinny PD (1996) The Itsaq Gneiss Complex of southern West Greenland; the world's most extensive record of early crustal evolution (3,900–3,600 Ma). Precambrian Res 78:1–39
Nutman AP, Bennett VC, Friend CRL, Rosing MT (1997) ~3710 and ≥3790 Ma volcanic sequences in the Isua (Greenland) supracrustal belt; structural and Nd isotope implications. Chem Geol 141:271–287
Nutman AP, Bennett VC, Friend CRL, Norman MD (1999) Meta-igneous (non-gneissic) tonalites and quartz-diorites from an extensive ca. 3800 Ma terrain south of the Isua supracrustal belt, southern West Greenland: constraints on early crust formation. Contrib Mineral Petrol 137:364–388
Nutman AP, Bennett VC, Friend CRL, McGregor VR (2000) The early Archaean Itsaq Gneiss Complex of southern West Greenland: the importance of field observations in interpreting age and isotopic constraints for early terrestrial evolution. Geochim Cosmochim Acta 64:3035–3060
Nutman AP, McGregor VR, Bennett VC, Friend CRL (2001) Age significance of U-Th-Pb zircon data from early Archaean rocks of west Greenland—a reassessment based on combined ion-microprobe and imaging studies—comment. Chem Geol 175:191–199
Nyquist LE, Shih CY (1992) The isotopic record of lunar volcanism. Geochim Cosmochim Acta 56:2213–2234
Oversby VM (1975) Lead isotopic systematics and ages of Archaean acid intrusives in the Kalgoorlie-Norseman area, Western Australia. Geochim Cosmochim Acta 39:1107–1125
Palacz ZA (1985) Sr-Nd-Pb isotopic evidence for crustal contamination in the Rhum intrusion. Earth Planet Sci Lett 74:35–44
Pankhurst RJ, Moorbath S, Rex DC, Turner G (1973) Mineral age patterns in ca. 3700 My old rocks from West Greenland. Earth Planet Sci Lett 20:157–170
Qiu Y, McNaughton NJ (1999) Source of Pb in orogenic lode-gold mineralisation: Pb-isotope constraints from deep crustal rocks from the southwestern Archaean Yilgarn Craton, Australia. Miner Deposita 34:366–381
Richards JR, Appel PWU (1987) Age of the "least radiogenic" galenas at Isua, West Greenland. Chem Geol 66:181–191
Rosholt JN, Zartman RE, Nkomo IT (1973) Lead isotope systematics and uranium depletion in the Granite Mountains, Wyoming. Geol Soc Am Bull 84:989–1002
Scherer E, Münker C, Mezger K (2001) Calibration of the lutetium-hafnium clock. Science 293:683–687
Schiøtte L, Compston W, Bridgwater D (1989) Ion probe U-Th-Pb zircon dating of polymetamorphic orthogneisses from northern Labrador. Can J Earth Sci 26:1533–1556
Schoenberg R, Kamber BS, Collerson KD, Eugster O (2002a) New W-isotope evidence for rapid terrestrial accretion and very early core formation. Geochim Cosmochim Acta 66:3151–3160
Schoenberg R, Kamber BS, Collerson KD, Moorbath S (2002b) Tungsten isotope evidence from ~3.8-Gyr metamorphosed sediments for early meteorite bombardment of the Earth. Nature 418:403–405
Stacey JS, Kramers JD (1975) Approximation of terrestrial lead isotope evolution by a two-stage model. Earth Planet Sci Lett 26:207–221
Stern RA, Bleeker W (1998) Age of the world's oldest rocks refined using Canada's SHRIMP: the Acasta gneiss complex, Northwest Territories, Canada. Geosci Can 25:27–31
Sultan M, Bickford ME, El Kaliouby B, Arvidson RE (1992) Common Pb systematics of Precambrian granitic rocks of the Nubian Shield (Egypt) and tectonic implications. Geol Soc Am Bull 104:456–470
Taylor PN, Kramers JD, Moorbath S, Wilson JF, Orpen JL, Martin A (1991) Pb/Pb, Sm-Nd and Rb-Sr geochronology in the Archean Craton of Zimbabwe. Chem Geol 87:175–196
Tera F (2000) Inference from the lead isotopes to the survival of a terrestrial crust 4.4 Ga old. American Geophysical Union Spring Meeting, Boston, V22B (Abstr)
Todt W, Cliff RA, Hanser A, Hofmann AW (1996) Evaluation of a $^{202}Pb$-$^{205}Pb$ double spike for high-precision lead isotope analysis. In: Basu A, Hart S (eds) Earth processes: reading the isotopic code. American Geophysical Union, Washington, DC, pp 429–437
Van Wyck N, Johnson CM (1997) Common lead, Sm-Nd, and U-Pb constraints on petrogenesis, crustal architecture, and tectonic setting of the Penokean orogeny (Paleoproterozoic) in Wisconsin. Geol Soc Am Bull 109:799–808
Villa IM, Kamber BS, Nägler TN (2001) Comment on: "The Nd and Hf isotopic evolution of the mantle through the Archean. Results from the Isua supracrustals, West Greenland, and from the Birimian terranes of West Africa". Geochim Cosmochim Acta 65:2017–2021
Wang LG, McNaughton NJ, Groves DI (1993) An overview of the relationship between granitoid intrusions and gold mineralization in the Archean Murchison Province, Western Australia. Miner Deposita 28:482–494
Whitehouse MJ, Kamber BS, Moorbath S (1999) Age significance of ion-microprobe U-Th-Pb zircon data from early Archaean rocks of West Greenland—a reassessment based on new combined ion-microprobe and imaging studies. Chem Geol 160:204–221
Whitehouse MJ, Kamber BS, Moorbath S (2001) Age significance of U-Th-Pb zircon data from early Archaean rocks of west Greenland—a reassessment based on combined ion-microprobe and imaging studies—reply. Chem Geol 175:201–208
Wiedenbeck M, Alle P, Corfu F, Griffin WL, Meier M, Oberli F, Vonquadt A, Roddick JC, Speigel W (1995) Three natural zircon standards for U-Th-Pb, Lu-Hf, trace-element and REE analyses. Geostand Newsl 19:1–23
Wilde SA, Valley JW, Peck WH, Graham CM (2001) Evidence from detrital zircons for the existence of continental crust and oceans on the Earth 4.4 Gyr ago. Nature 409:175–178
Wooden JL, Mueller PA (1988) Pb, Sr, and Nd isotopic compositions of a suite of late Archean igneous rocks, eastern Beartooth Mountains—implications for crust-mantle evolution. Earth Planet Sci Lett 87:59–72
Zartman RE, Haines S (1988) The plumbotectonic model for Pb isotopic systematics among major terrestrial reservoirs—a case for bi-directional transport. Geochim Cosmochim Acta 52:1327–1339